Published by :
http://www.ijert.org

International Journal of Engineering Research & Technology (IJERT)
ISSN: 2278-0181
Vol. 14 Issue 03, March-2025

Prognostication of Ground Subsidence Problem in Joshimath Hill Slope Through Characterization of Soil

Harish Bahuguna, Megotsohe Chasie, Dhananjai Verma, Sebabrata Das,
Yogendra Singh, Tahir Mushtaq, A. K. Mishra
Geological Survey of India, Central Headquarters Kolkata, Geological Survey of India, State Unit Maharashtra, Pune, Ministry of Mines Government of India, New Delhi, Geological Survey of India, State Unit Uttarakhand, Dehradun

ABSTRACT
The Higher Himalayan region is geologically fragile and tectonically active and it has suffered a number of natural disasters like flooding, GLOF and landslides in the past and the fate has not changed even in the present time. The hill slope, over which Joshimath agglomeration is located, is constituted of a thick pile of debris of an old slide which took place in the later part of nineteenth century AD and was well published in the Himalayan Gazeteer of 1866. The urban sprawl has grown from a small village to a township with a population of more than 22000 people and 2364 buildings, many of the buidings are of commercial nature. The Joshimath area had been experiencing ground subsidence problem for the last more than five decades and the unabated construction activities have only exacerbated the stability conditions on the hill slope. The incidence of sudden burst of silt laden water seepage with an initial discharge of 600 litre per minute was accompanied/followed by appearance of tension ground cracks in the middle and lower part of the hill slope forcing the authorities to relocate many people. A comprehensive and detailed geological and geotechnical investigation was carried out with an aim to identify and prognosticate the stability of the hill slope and the outcomes of geotechnical investigations of soil properties/parameters with their relationship/bearing on the ground subsidence/distress features in Joshimath, has been brought out in a methodical and scientific manner and the results will facilitate the policy planners to mitigate the problem of ground subsidence.

1. INTRODUCTION

Landslides inter-alia ground subsidence's are omnipresent across the globe, in any terrestrial environment and have an important part in the evolution of landscape [1] yet they pose a serious threat to populations [2]. Landslides are driven by various forces such as tectonic, climatic or anthropogenic activities [3,4, 5]. International Disaster Database (EM-DAT) suggests that as compared to other natural disasters, the landslides account for 4.9% of all natural disasters and 1.3% of all natural hazard fatalities between 1990 and 2015 and out of all landslides nearly 54% occurred in Asia [6]. One of the primary causes of landslides is human activity that includes deforestation, excavation of slopes for construction and development in unstable hillside areas due to population growth and urbanization [7].

Ground subsidence is quite common in a number of hill towns located in different parts of the globe and so is the case in Higher Himalayan region [8, 9]. Scarcity of space to accommodate the growing demands of more houses/buildings/hotels and the infrastructural facilities pose a serious challenge before the government and the civic authorities [10]. The challenge becomes more so daunting in the face of the ensuing climate change impacts, the fragile geological and ecological system. Joshimath area, located at about 230 km from Rishikesh (nearest railhead), is approachable through an all-weather metalled road (NH-58). It is an important urban centre, with a historical background, in the Higher Himalayan zone in the state of Uttarakhand, India. The urban sprawl is spread over nine wards, namely Gandhinagar, Marwadi, Singdhar, Manoharbagh, Upper Bazar, Lower Bazar, Sunil, Parsari, and Ravigram, [11,12] and the boundaries of this town are defined by Alaknanda River (north), Auli (south), Parsari Nala (east) and Marwadi (west). The entire hill slope between Auli and Alaknanda River, is occupied by a thick pile of palaeoslide debris which is heterogeneous in nature, and it is also dotted by several springs (indicating the presence of shallow water table or perched water tables). The ground elevation varies from 1332 m to 3229 m with a maximum elevation near Auli and a minimum at the Alaknanda River bank.

It is mentioned in the historical annals that Joshimath is located on landslide debris [13] and in their monograph brought out in 1936, [14] reported that Joshimath town is located on an old landslide deposit that was triggered at an

International Journal of Engineering Research & Technology (IJERT)
ISSN: 2278-0181
Vol. 14 Issue 03, March-2025

elevation of ~4000 m east of Kuari Pass, and the slopes between Joshimath town and Tapovan were burdened with massive boulders [14]. The issue of ground subsidence in Joshimath area came into prominence when a high-level committee was formed in 1976 under the chairmanship of Sh. M. C. Mishra, the commissioner of Garhwal which gave its detailed report on the ensuing problem and suggested comprehensive mitigations measures for the Joshimath town [15]. However, most of the recommendations of Mishra committee report could be implemented on ground and Joshimath area kept experiencing the incidences of ground subsidences in 2005, 2008, 2012, 2013, 2015, 2021 and 2022 [16,17, 18].

Joshimath town has grown from a small village having hardly a dharmshala/lodge [17] to a bustling town of over 230000 people and over 2364 buildings out of which nearly 91% i.e., 2,152 buildings were houses and rest were either government buildings or commercial ones, a majority of these i.e., more than 62% of these buildings are more than 2 storeys [19]. The ever-increasing load of these structures on vulnerable hill slopes in fragile Higher Himalayan terrain exacerbate the problem of slope instability more so in a town like Joshimath which is experiencing the problem of ground subsidence for the past five to six decades [14,15,16,17,18] and posing a serious threat to the people inhabiting such areas [20]. The scenario becomes really scary when 99 %of all the buildings are non-engineered i.e., non-compliant to the provisions of National Building Code of India 2016 [19] in a seismotectonically highly sensitive terrain liying in seismic zone V [21] where earthquake events of Mm 7 or more are expected.

There was an unusual incidence of sudden outburst of silt-laden water with an initial discharge of 600 litre per minute [11] in the early hours of 2nd January 2023, from Marwari area, located in the lower part of the Joshimath hill slope and it was followed by ground subsidence marked by the appearance of new ground cracks between Marwari – Singdhar – Manohar Bagh and Sunil Gaon areas of Joshimath. These ground distress features inflicted a widespread damage to more than 500 buildings and other civil structures inter-alia hotels and lodges. Some of the hotels and household buildings were severely damaged and it compelled the local authorities to relocate the people to safer areas.

Several studies have identified the geotechnical properties of soil and rock and slope stability factors that contribute to the primary cause of landslides, including landforms, hydrological conditions, and relief [22,23,24,25,26,27,28,29,30,31,32]. In recent years, spatially variable soil thickness maps have frequently been incorporated in distributed slope stability modeling [33,34,35], but geotechnical and hydrological parameters have been proven to be more troublesome to manage because they are characterized by an inherent variability and their measurement is difficult, time-consuming, and expensive, especially when data is needed for large areas [36, 37,38]).

The geotechnical parameters of soils were determined by a series of in situ and laboratory tests, as because the field tests are more difficult to manage and control than laboratory tests, but they are considered to give a more direct and representative measurement of the real in situ soil properties [39]. Present study has referred the data from the in-situ testing of soil in Joshimath area from the reports of Indian Institute of Technology Roorkee [40] and National Geophysical Research Institute Hyderabad [41]. Generally, Geology, Geomorphology, climate and anthropogenic activities are considered as primary factors controlling the stability of a slope [42] but geotechnical characterization of debris material/soil shows that the fine-grained particles diminish the engineering geological parameters of the slope material and consequently weaken the slope stability [43,44,45].

The physical properties of soil, such as bulk density, cohesiveness and shear strength have been noted to affect stability of disturbed soil [46,47,48,49]. However, the most problematic soils comprise of expansive, soft clay, collapsible and dispersive soil which may induce slope failure, due to their distinct shrink-swell properties at various moisture content [50,51]. The percentage of clay size particles, in particular gives clear indication to the nature of the soils while the determination of Atterberg limit is an important component of soil analysis particularly in terms of its expansion at the different moisture and clay contents [52]. Well graded soil provides greater shear strength over poorly graded soil with clay content whereas the studies by [53,54,55] showed that increase in the percentage of finer material tends to increase the slope instability and hydrophilic clay minerals develop a specific lubrication constitute risk of slope stability. Fine grained clay particles retain the fluid which increases the shear stress through the pore pressure which consequently reduces the effective stress and leads to instability [42,56,57]. A reduction in inherent shear strength of slope material augments slope instability [42,58,59].

2. RESEARCH GAP

Various researchers have worked on different aspects of ground subsidence noticed in Joshimath area and have touched upon different site investigations like geological, geophysical and geotechnical investigations. These studies have brought out details about ground characteristics and material properties of bed rock and soil viz strength characteristics of bed rock, shear parameters of the soil, porosity, permeability, degree of saturation and bearing

International Journal of Engineering Research & Technology (IJERT)
ISSN: 2278-0181
Vol. 14 Issue 03, March-2025

capacity of soil in different parts of Joshimath. However, none of the studies have been comprehensive in the sense to put forward a plausible scientific reasoning for the ground distress features vis-à-vis soil properties in Joshimath area. It has been well published by many workers that Joshimath hill slope consists of a plaeoslide material and there is a problem of ground subsidence for at least the last five decades but none has addressed the moot points such as i) not all the area on the hill slope of Joshimath was/has been affected by ground subsidence/distress, ii) why only certain parts are getting affected by subsidence and what differentiates them, iii) the nature of ground distress features is not same even in the affected parts i.e. somewhere it is subsidence related tension cracks and at other places the distress is confined to the flanks of natural drainages or on the edge of the contour terraces, iv) why the western part of the middle hill slopes is dotted with number of springs while the eastern part shows development of drainage channels v) is there variation in the contents of the soil/overburden material in different parts of the hill slope and vi) to what extent the difference in the physical and geomechanical properties of the soil/overburden have influenced the ground subsidence.

Every other study for Joshimath hill slope stability or on the analysis of ground subsidence phenomenon speaks about the spatial distribution of ground cracks but our present study throws an important light on the temporal distribution of the various ground distress features/cracks apart from their spatial locations. Another diagnostic and unique aspect that this present study highlights is the characterization of the pattern of these ground cracks with respect to their spatial location. The spatio-temporal position of the ground distress features has been superposed with the disposition of different types of soils in different parts of the hill slope and then the physical, geotechnical, shear and geotechnical parameters were superposed to get a direct comparison between the material characteristics of the soil and the typology of the ground cracks.

This paper specifically aims at addressing this evident research gap and for the first time brings out a detailed scientific study comprising of geological, geotechnical, detailed material characteristics and their relationship with the ensuing ground deformations/ground subsidence problems in different parts of Joshimath.

3. METHODOLOGY

Standard Operating Procedure (SOP) on mesoscale (1:5,000 scale) landslide susceptibility mapping of Geological Survey of India [60] has been used as a base methodology for this particular study with relevant modifications. The pre-field study mainly involved literature survey along with collection of basic datasets for field study. LiDAR survey provided by Uttarakhand State Disaster Management Authority (USDMA) was utilized for preparing a very high-resolution Digital Elevation Model (DEM) of Joshimath Township and topographical map with 2 m contour interval so prepared served as the base map for the field study. Realtime Kinematic (RTK) Survey through digital ground positioning system (DGPS) was utilized for the recording of key ground features like seepages, springs, surface drainage, ground cracks, configuration of overburden material etc. were mapped using. The samples of soil from different slope forming material were collected from site to determine geotechnical properties. Geotechnical analysis of the undisturbed and disturbed soil samples collected from different parts of Joshimath hill slope was carried out in the laboratory. The results of geotechnical properties of soil as determined through lab were compared with the results of grain size analysis and shear parameters as determined through multiple channel analysis of surface waves (MASW) and dynamic cone penetration test (DCPT) done by Indian Institute of Technology Roorkee (IIT R) and those determined through AVRI, MASW and ground penetration radar (GPR) survey by national geophysical research institute (NGRI). The distress features in different parts of Joshimath hill slope were categorized based on their typology, nature, spatial position and physical attributes like orientation, continuity, linearity and opening. Finally, the results of soil classes along with their geotechnical characteristics were overlaid with the spatial position of ground cracks to decipher the relation between soil characteristics and the ground distress features.

International Journal of Engineering Research & Technology (IJERT)
ISSN: 2278-0181
Vol. 14 Issue 03, March-2025

Table-1: Data Source used for the study

Geo-factor Maps/Layers	Data Source	Data availability
Lithology and fault/thrust	Bhukosh portal of the Geological Survey of India	Open-access data is available at https://bhukosh.gsi.gov.in/Bh ukosh/MapViewer.aspx
Drainage map	HydroSHEDS database	https://www.hydrosheds.org/
Slope angle, Slope Aspect, Slope Curvature, Relative Relief, Terrain Roughness Index, Geomorphon	Shuttle Radar Topography Mission (SRTM) Digital Elevation Model (DEM)	Open-access data is available at https://earthexplorer.usgs.gov
Land use land cover (LULC)	Sentinel-2 10m Land Use/Land Cover	Open-access data is available at https://livingatlas.arcgis.com /landcoverexplorer
Landslide Inventory	Polygon datasets of landslides downloaded from the Bhukosh portal of the Geological Survey of India	Open-access data is available at Geological Survey of India https://bhukosh.gsi.gov.in/Bhkosh/MapViewer.as px
Ground Deformation Features, Seepage points	RTK Survey	Chasie et. al. 2024
Grain Size and Shear Strength Characteristics through MASW, DCPT	Geotechnical Investigations by Indian Institute of Technology (IIT) Roorkee	https://usdma.uk.gov.in/PDFFiles/IITR.pdf
AVRI, GPR data	Report of National Geophysical Research Institute (NGRI)	https://usdma.uk.gov.in/PDFFiles/NGRI.pdf

4. GEOLOGY OF THE STUDY AREA

Joshimath town is located within the Uttarakhand segment of the active Himalayan Fold-Thrust Belt (FTB) [61,62,63,64] and forms part of the Higher Himalaya which is bounded between South Tibetan Detachment Surface (STDS) towards north and Main Central Thrust (MCT) towards south. The rocks in the study area belong to Helang and Mana formations of Central Crystalline Group of rocks of Paleaoproterozoic age (Fig. 1). The Helang Formation is comprised of granite gneiss, mylonite gneiss, augen gneiss, quartzite, quartz mica (±chlorite) schist and minor marble and basic rocks whereas the rocks of Mana Formation consist of streaky banded/augen gneiss, migmatite, kyanite schist, garnetiferous mica schist, quartzite, calc silicate and marble bands (Source: 1:50K map of GSI, www.gsi.gov.in).

4.1. GEOMORPHOLOGY

A prominent geomorphic feature within the study area is the N-S trending spur from Auli to Alaknanda, which is parallel to the western escarpment of the area and it divides Joshimath town into western and eastern parts which comprises 32.72% and 23.95% of the total mapped area respectively .Interestingly the eastern part of the study area is represented by closely spaced network of channels and streams whereas the western part is dotted with number of seepages and springs and this has an important bearing on controlling the slope deformation (Fig. 2).

International Journal of Engineering Research & Technology (IJERT)
ISSN: 2278-0181
Vol. 14 Issue 03, March-2025

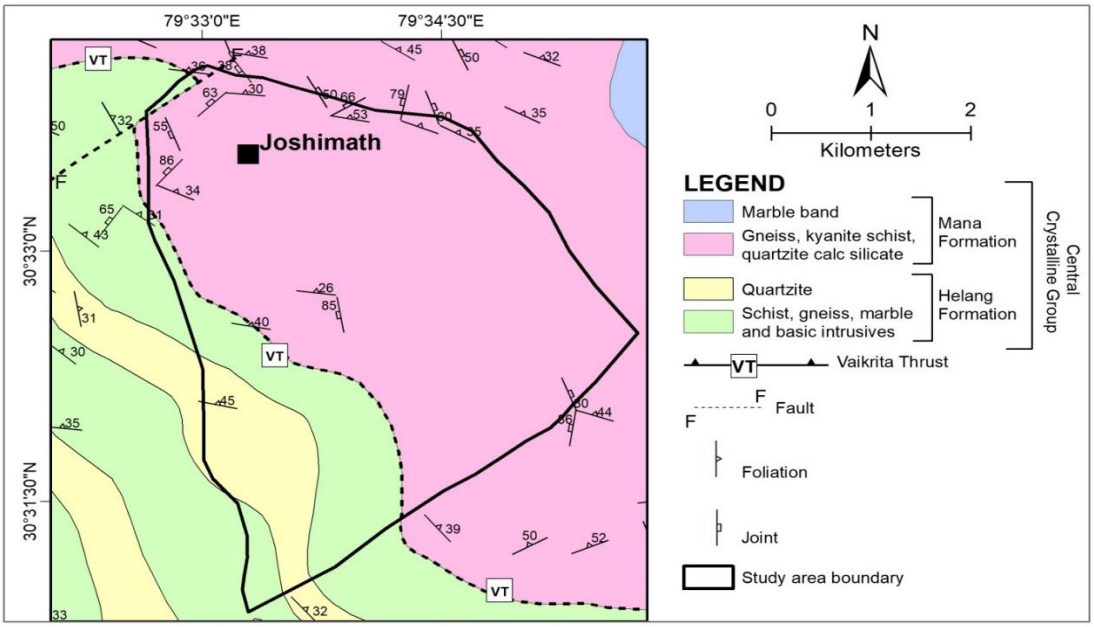

Fig. 1: Geological map of the area selected for present study (Source: 1:50K map of GSI).

4.2. DETAILED GEOLOGICAL MAPPING

The detailed geological mapping of about 17 km^2 area in and around Joshimath Township was carried out on 1:5,000 scale (Fig. 3) delineating the bedrock exposures with its structural elements and also brought out the rock-overburden contact. Ground observations during the detailed geological mapping helped in classifying the overburden material into different classes, recording of natural drainages and seepage points, recording and delineation of various ground distress features and mapping of different clusters of big boulders on the hill slope. A number of geological sections, both along the slope direction and across it, were developed to find out the distribution of geological formations, overburden and the ground distress features (Fig. 4a,b,c and Fig. 5a,b,c). The geological profiling coupled with the data of geophysical profiling through electrical resistivity (ERT) survey and the one with Ground Penetrating Radar (GPR) as taken from the report of National Geophysical Research Institute (NGRI), has enabled the authors to estimate the tentative depth of overburden on the hill slope. It has been found that the thickness of the overburden is variable in different parts of the slope with the maximum of about 100m being in the middle and lower part of the slope mainly to the west of the geomorphic high i.e. Singdhar high whereas the minimum thick ness varying between 1m and 4m was found in the extreme upper part of the slope (Auli area), along the flanks of AT nala and Parsari nala on the eastern margin of the study area and in the extreme lower part of the slope near Alaknanda River.

Published by :
http://www.ijert.org

International Journal of Engineering Research & Technology (IJERT)
ISSN: 2278-0181
Vol. 14 Issue 03, March-2025

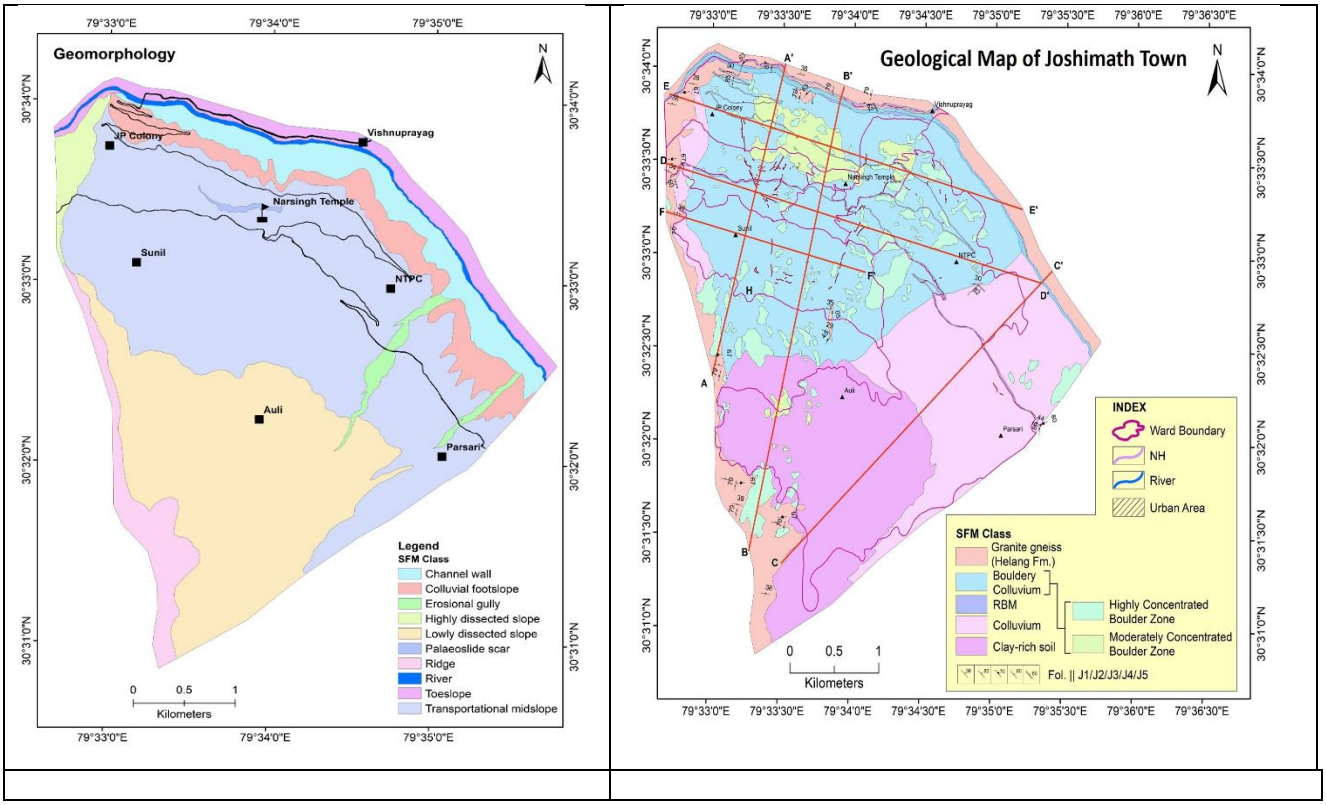

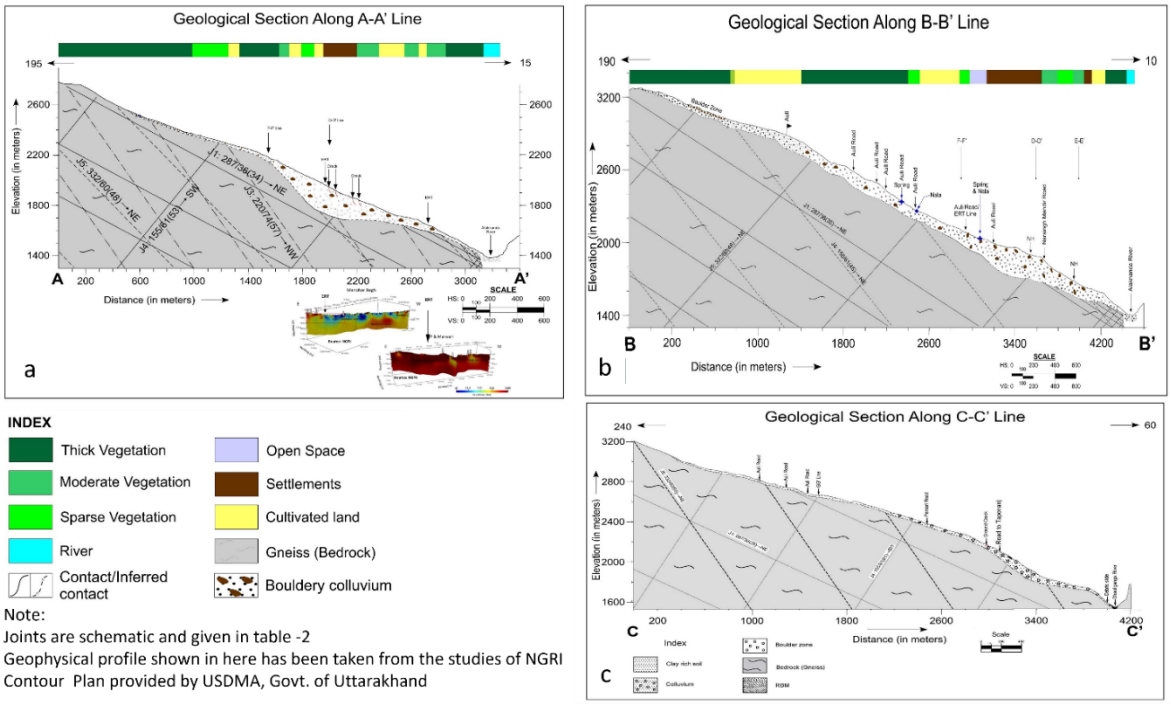

Fig. 4: a) Geological section along A – A' Line, b) Geological section along B – B' Line, c) Geological section along C – C' Line, e) Geological section along D – D' Line, f) Geological section along E – E' Line, g) Geological section along F – F' Line

Published by :
http://www.ijert.org

International Journal of Engineering Research & Technology (IJERT)
ISSN: 2278-0181
Vol. 14 Issue 03, March-2025

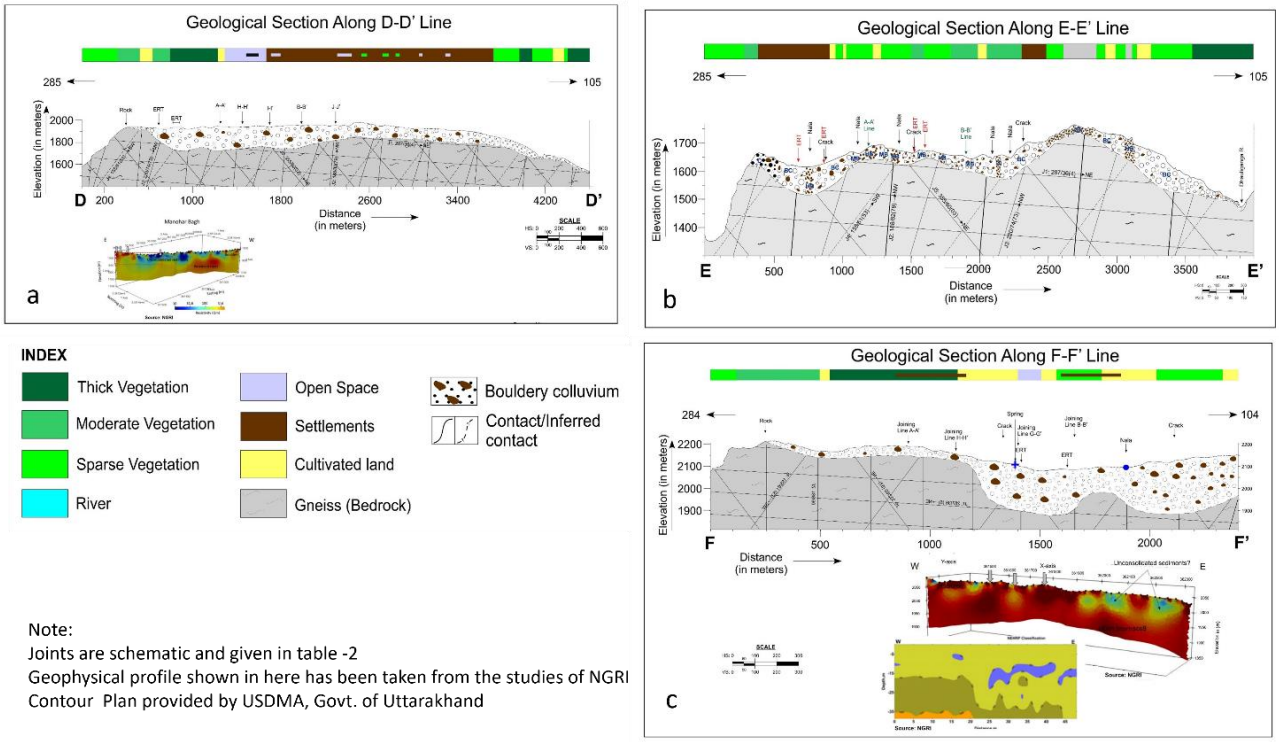

Figure-5: a) Geological section along D – D' Line, b) Geological section along E – E' Line, c) Geological section along F – F' Line

4.2.1. BEDROCK :The granite gneiss with thin bands of quartzite and calc-silicate rock belonging to Mana and Helang Formations of Central Crystalline Group is exposed in and around Joshimath town with scanty exposures . However, the bedrock is exposed all along the western margin starting from Auli ridge down to the Alaknanda River (Fig. 3). In continuity of these western margin exposures, the bedrock is exposed at the toe of the Joshimath slope i.e .on the left bank of Alaknanda River near Marwari Bridge, and these exposures extend up to 150m in the upstream direction (Fig. 3). A small patch of bedrock is also seen exposed below Kamath-Chunar area and Vishnuprayag area. In the mid slope, the rock exposures are found below the Auli area along N-S slope divide, in the lower part of AT nala and lower-middle part of Parsari nala on Joshimath-Malari Road .

The rocks in the area have five sets of prominent joints including foliation joint the fabrics of the joint sets are tabulated in Table-2 and their plot in rose diagram and corresponding π-diagrams are shown in Fig.–6A –6E. The presence of wide opening up to 1m along joint planes were observed along the Alaknanda River at many places and these joints were often filled with overburden material.

Table -2: Details of the joint set parameters.

Joint	Dip	Direction	Spacing	Continuity	Aperture	Remark
F-J1	25°-64°	5°-45°	3-25cm	>5m	Tight	RU
J2	55°-86°	260°-284°	4-40cm	1-1.5 m	Open	RU
J3	63°-86°	292°-330°	5-21cm	1-5m	Tight	RU
J4	38°-70°	185°-250°	20-150cm	2-3m	Open	RU
J5	50°-80°	30°-75°	8-42cm	1-3m	Open	RU

International Journal of Engineering Research & Technology (IJERT)
ISSN: 2278-0181
Vol. 14 Issue 03, March-2025

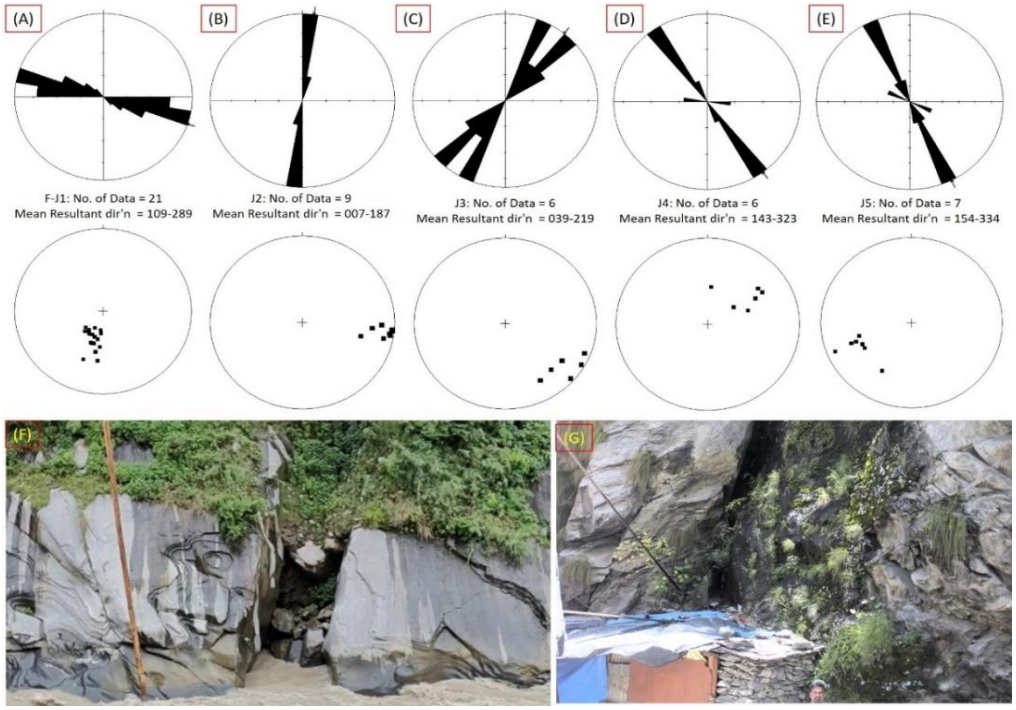

Fig. 6. Rose diagram of Joint plane data along with respective π-diagrams to visualize the dip component: (A) Foliation Joint (F-J1), (B) Joint-2 (J2), (C) Joint-3 (J3), (D) Joint-4 (J4) and (E) Joint-5 (J5), (F) Opening along joint in bedrock filled with overburden material near Vishnuprayag; (G) Opening along joint near Marwari bridge.

5. GROUND DEFORMATION CHARACTERIZATION

An unprecedented incidence of sudden burst of water in the lower part of hill slope at Jaypee Colony, in Marwadi ward occurred in the early hours of 2nd January 2023 and this burst of water was followed by ground subsidence in the lower and middle part of the hill slope. The ground deformation features were mapped using a very high-resolution (0.25 m) Digital Elevation Model (DEM) of Joshimath Township with 2 m contour interval and with the help of DGPS instrument by employing Real Time Kinematics (RTK), which was first calibrated with base station points used for topographic survey. The boundaries of the geo-factors responsible for ground cracks/ fissures and other deformations have been delineated signifying the role of class and subclass of various geo-factors likely to be responsible for the processes. During the detailed geological mapping not only the ground cracks and subsidence features of 2nd January 2023 were recorded but all the other distress/deformation features/signatures on the ground were mapped (Fig. 7a - e). The typology of different ground distress features was studied in detail and after a thorough examination and understanding of the nature and characteristic features, all the ground deformations in the area were categorized into four classes i.e. i) ground cracks/ fissures, ii) subsidence along road and settlement areas, iii) debris slides and iv) old landslide scars. To make this typology more specific the spatial and temporal attributes about these distress features were also well defined and based on the spatial occurrence three patterns of ground cracks were defined. Pattern-1 (Associated with Ground subsidence) are the ground cracks which were a result of sudden draining of the matrix of slope forming material, aligned NNW-SSE and confined to the western side of the geomorphic high (Singdhar high; Fig. 7) in the middle and lower part of the hill slope as recorded in Marwari-Singhdhar-Manoharbagh-Sunil Gaon area and have limited linear extent along the slope. The Pattern-2 ground cracks are also aligned NNW-SSE to NNE-SSW largely confined on the fringe areas flanking the valleys of nalas descending from Auli to Alaknanda River. These are a result of natural process of valley widening along 2nd and 3rd order channels in such hilly terrain. Such as AT nala, Parsari nala and the nala flowing close to Narsingh Mandir. The Pattern-3 (Slips along free faces of the slope) ground cracks have been recorded on the margins of the terraces or road benches, are also a result of natural process of sliding along the free face in hilly terrain. For a temporal categorization the event of ground subsidence of 2nd January 2023 was chosen as the bench mark and the cracks existing before the event and after that event were temporally segregated and the former were categorized as old while the latter as new cracks.

Published by :
http://www.ijert.org

International Journal of Engineering Research & Technology (IJERT)
ISSN: 2278-0181
Vol. 14 Issue 03, March-2025

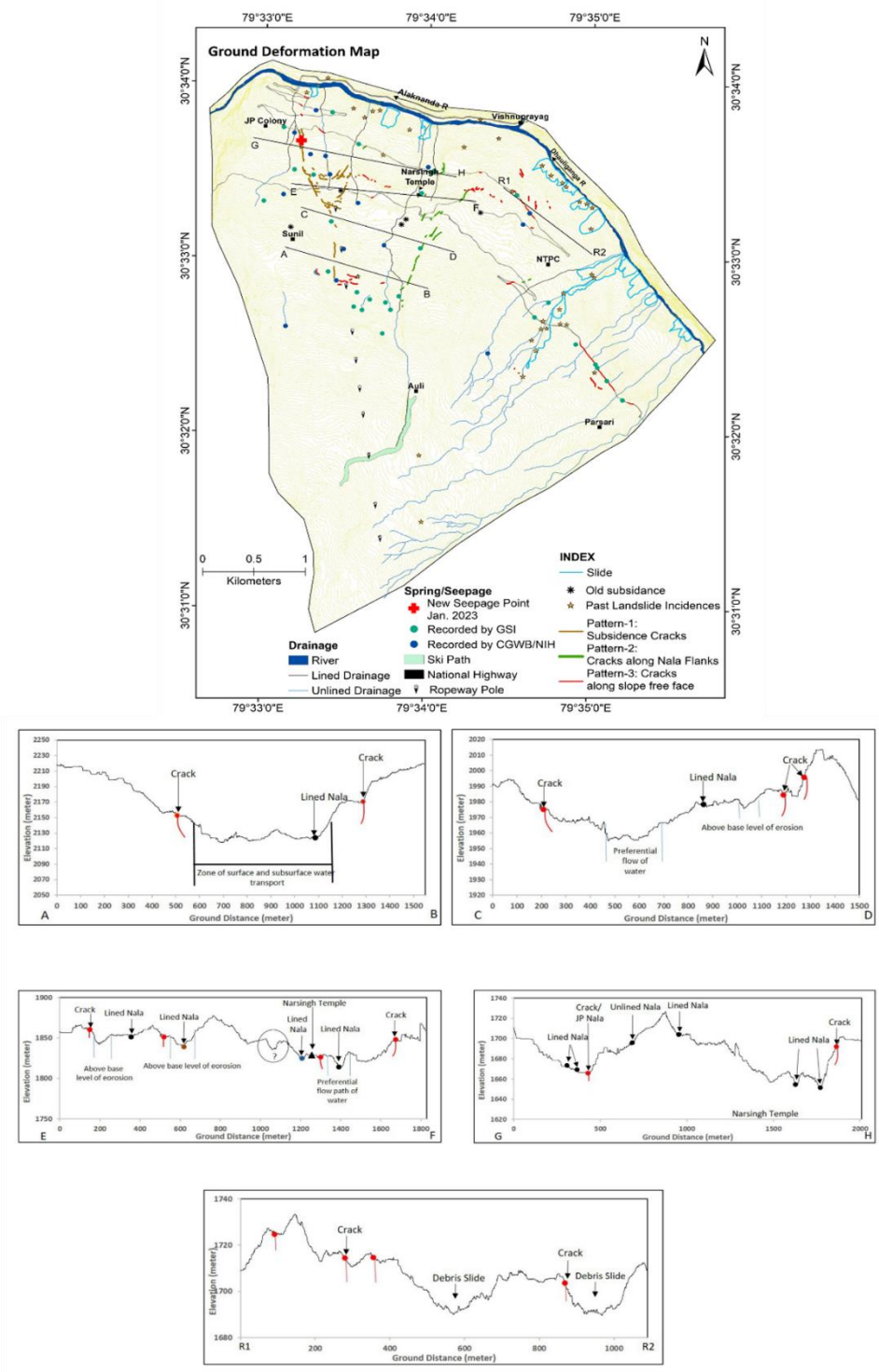

Fig. 7, a) Ground Deformation Map of Joshimath Area, b) Cross Profile along A – B section showing position of Ground Cracks, c) Cross Profile along C – D section showing position of Ground Cracks, d) Cross Profile along E – F section showing position of Ground Cracks, e) Cross Profile along G – H section showing position of Ground Cracks, f) Cross Profile along R1 – R2 section showing position of Ground Cracks

International Journal of Engineering Research & Technology (IJERT)
ISSN: 2278-0181
Vol. 14 Issue 03, March-2025

The NNW-SSE trending linearity in the ground cracks at the western part of study area starts from Jaypee colony located in Marwadi ward and continues south-easterly (upslope) passing through Singdhar, Manoharbagh and up to Sunil gaon area (Fig. 7) and the damage caused by the ground cracks increases towards downslope while the maximum damage was observed in Manoharbagh area. The NNE-SSW oriented linear cracks located in the central part of study area starts from Gandhinagar ward and continues in southwesterly direction passing through Ravigram up to Sunil ward (Fig. 7a-e). This zone has developed transverse ground cracks, which are retrograding towards upslope marked by development of new ground cracks. The depth of the cracks observed in the agriculture land is up to 1.5 m with horizontal displacement of 30-60 cm.

6. GEOTECHNICAL INVESTIGATIONS

The physical and geomechanical properties of slope forming material are one of the major contributing factors for guiding the behavior of these materials for a given slope and hence they play a key role in evaluating/ assessing the stability of any given slope. The slope forming material (SFM) in the study area as brought out during the course of large scale geological mapping on 1:5000 scale, mainly consisted of clay rich soil in Auli area, colluvium with different concentration of boulders in main Joshimath Township area, colluvium in Parsari area and scarcely exposed bedrock. The bedrock exposures are present in the mid slope near Auli, on the flanks of Parsari nala, western escarpment and on the banks of Alaknanda River. In view of the distribution of different SFM, 05 nos. of bedrock samples, 32 nos. of undisturbed samples and 13 no. of disturbed samples representing matrix of different classes of SFM have been collected. The geotechnical parameters of these collected samples were determined at the Geotechnical Laboratory, GSI, NR. The spatial distribution of these samples in study area is presented in Figure 8 and in Table 4 and interpretation of their geotechnical parameters are discussed in the section given below.

6.1. BEDROCK SAMPLES

In view of the scanty exposures only five no. of samples from different locations were collected (Fig 8). Utilizing the Deerie Miller approach and the field attributes of joint surfaces the assessment of rock mass class through rock mass rating (RMR) indicates the RMr rating values of the gneisses varying from 37 to 85 indicating fair to very good category of rock mass. The Uniaxial Compressive Strength (UCS) values for the samples are calculated through empirical relationship of point load and the values have been discussed in the results.

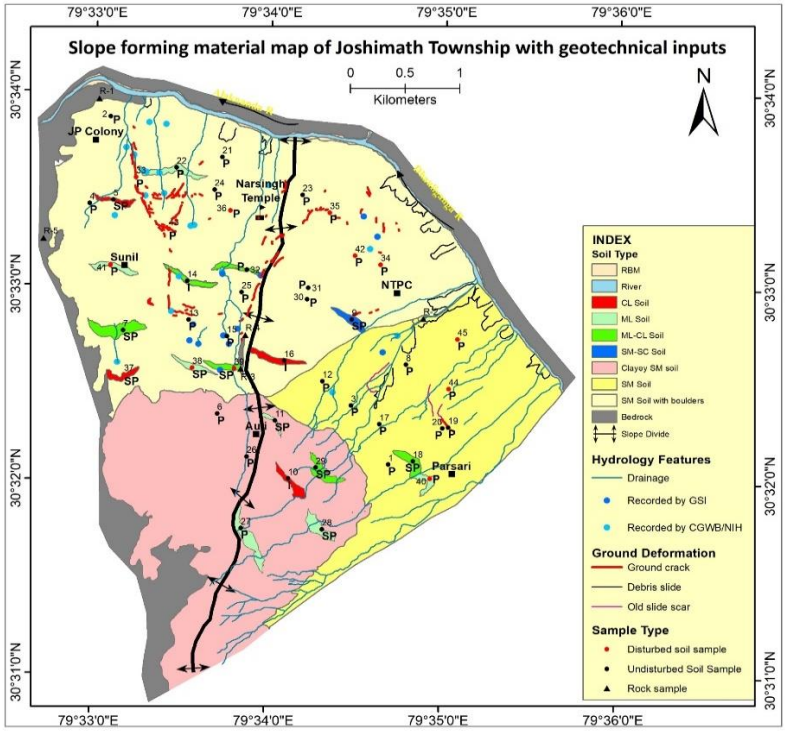

Fig. 8. Slope forming material map with inputs from soil classification based on USCS along with spatial distribution of different rock and soil samples and location of goetchnical samples. (Symbols used SM: Sand silt mixture; SM-SC: Clayey sand-silt mixture; ML: Silty or clayey fine sand; ML-CL: Silty or clayey fine sands; CL: Sandy clays; P: Pervious; SP: Semi Pervious; I: Impervious).

International Journal of Engineering Research & Technology (IJERT)
ISSN: 2278-0181
Vol. 14 Issue 03, March-2025

6.2. SOIL SAMPLES:

The soil/overburden material in the study area is highly heterogeneous in nature and on the basis of field observations it was classified in highly and moderately concentrated boulder zone, bouldery colluvium, colluvium and clay rich soil. The soil samples were collected from a grided pattern of 500m×500m grid carefully avoiding the influence of anthropogenic activity and other influences like extensive dissections, seepage, natural spring etc (Photo-1). As such the area does not show a complete soil profile development but for a clay-rich soil in the upper reaches of hill slope around Auli area where C-Horizon of soil profile is well developed.

Photo-1: Undisturbed soil sample collection in GI pipe after removal of top organic layer

6.2.1. Grain size analysis: Grain size analysis is widely used in classification of soils [65] and the grain size distribution test is generally carried out using sieves [66,67,68]) and hydrometer [69]. To determine the grain size and grain size distribution, sieve analysis was performed and samples were classified following the Unified Soil Classification System (USCS) [70]. The classification of soil samples suggests mainly two groups i.e., coarse grained sandy matrix and fine-grained silt and clayey matrix which were further classified in different classes based on plasticity chart. The grain size curve gives important information on (i) the total percentage of larger or finer particles than a given size and (ii) the uniformity or the range in grain-size distribution. Coarse grained soils are generally classified on the basis of the grain size distribution, and fine grained soils based on Atterberg limits which take into account the soil plasticity. A well graded soil exhibits a wide range of grain sizes present in it whereas coarse grained soils failing to meet these criteria are classified as poorly graded soils including uniformly graded soils and gap graded soils.

6.2.2. Grain Size Distribution

A set of sieves is used for separating the different sizes of coarse grained (gravels and sands) soils and a hydrometer is used on the fine grained (silts and clays) soils. D10, D15, D30, D50, D60, D85 are some of the common grain sizes derived from the grain size distribution curve for soil classification, designs of filters and vibro-flotation. D10 grain size corresponds to 10 % passing meaning thereby that 10 % of the grains in the tested soil sample are smaller than this size. It may be emphasized here that D10 is effective grain size, which reflects the size of the pore channels that are capable of conducting water through soils. Similarly, D50 is the median grain size which means that 50 % of the grains are larger than this size, which is different from the mean grain size.

Coefficient of uniformity (Cu) and coefficient of curvature (Cc) are two important indicators for assessing the geometry of a particular soil and it's grading which in turn has bearing on the size of intergranular pore spaces and the internal stability of the soil grains. The spread of the grain sizes within the soil is reflected in the magnitude of the coefficient of uniformity (Cu) which is expressed as defined as:

$$Cu = D60 / D10$$

Cu is always greater than unity and a value close to unity implies that the grains are about the same size. A value of $C_u > 6$ indicates a densely graded (i.e. well-graded) material with a considerable range of particle size (used for max stability). $C_u < 4$ indicates a uniformly graded (i.e. open-graded) material having a narrow range of particle size (used for max permeability).

International Journal of Engineering Research & Technology (IJERT)
ISSN: 2278-0181
Vol. 14 Issue 03, March-2025

The other parameter used for classifying granular soils is a dimensionless parameter known as the coefficient of curvature or coefficient of gradation (Cc) which describes the shape of the grain size distribution curve of soil. It provides an important insight into the uniformity and gradation of soil particles and helps in understanding the behavior and properties of any soil.

$$Cc = (D30)^2 / (D10 \times D60)$$

Soils exhibiting Cc values in the range between 1 and 3 are generally considered well-graded, however, it should also satisfy the criteria of *Cu* value greater than 6 and in that case, it would indicate that these soils have a good mix of different particle sizes that fit together tightly when compacted. In case a particular soil sample shows a single size of grains the for this sample the value of both Cu and Cc should be 1.

6.2.3. Relation between internal stability and Cc

The internal stability of a given soil pertains to the ability of its coarse fraction to prevent the loss of its fine fraction due to seepage flow [71] and vice versa if the fine fraction is lost due to flow of water, the soil is considered internally unstable. Internal stability of a soil is largely governed by the grain sizes and their distribution, pore sizes and their distribution and constriction sizes, hydraulic gradient, flow velocity and flow direction compaction efforts and cohesion [72,73,74,75]. Coarse soils with a flat tail of fines and gap-graded soils are often internally unstable [76]. A well-graded soil with less than 5% fines is internally stable provided it satisfies (H/F) min > 1.0 (F= mass fraction of particles finer than grain size d, H = mass fraction of particles ranging from d to 4d). All the sources have been tabulated in Table-3 for the evalution of graded soil. On the other hand, a gap-graded soil having fine particles less than10% is internally stable subject to the fact that its gap ratio should be less than 3.0. A well-graded soil with a fines content of more than 20% or a gap-graded soil with a fines content of more than 35% is deemed to be internally stable [71].

Table-3: Source for Evaluating the Grading of the Soil

Soil Type	**Criteria**	**Source**
All soils	(d15c/d85f)max≤4: internally stable	[77]
Well-graded soils	30/log(d90/d60)o80, or – 30/log(d90/d60)o80 and15/log(d20/d5)422 internallystable	[74]
Granular soils	(H/F)min≥1.0: internally stable	[72]
Granular soils	For F<15, (H/F)min≥1.0; internally stable For F>15, H≥15; internally stable	[78]
Sandy gravel	Cu≤10: internally stable 10≤Cu≤20: transitional Cu≥20: internally unstable	[79]
Cohesion-less and graded soils	0.76log(h″)+1oh′o1.68 log(h″)+1: internally stable	[80]

6.2.4. Specific Gravity: The specific gravity for various classes of soil in the study area varies from 2.46-2.73 for SM class, 2.58 for SM-SC class, 2.59-2.72 for ML class, 2.56-2.67 for ML-CL class and 2.59-2.64 for CL class (Table-5). The relative study of grain size distribution with specific gravity suggest that the specific gravity of samples is directly proportional to the sand proportion and inversely proportional to the silt+clay proportions. The specific gravity of one sample (JDSS10) in Ravigram area in the northeastern part of hill slope is significantly low as compared to other samples. It is worth mentioning that some workers have reported a linear relation between specific gravity and the shear strength parameters (C and Φ) of the soil [81] the same for Joshimath samples has been reflected in the discussions.

6.2.5. Wet and Dry Density: The wet density is a measure of the mass of matrix plus liquids divided by the volume as a whole whereas the dry density is a value that represents the density of matrix in dry state. The measurement of wet and dry density was done for undisturbed soil samples (DSS) only (Table-6). The highest value of 2.05 gm./ cc wet density was found in SM and ML-CL classes, whereas, the highest value of 1.82 gm./ cc of dry density was found in SM class. Overall, the relative study of grain size proportion in individual samples along with different symbol classes of USCS does not lead to any conclusion that can lead to show any relation with change in wet and dry density of analysed sample.

International Journal of Engineering Research & Technology (IJERT)
ISSN: 2278-0181
Vol. 14 Issue 03, March-2025

6.2.6. Void Ratio, Porosity and Permeability:

In a heterogeneous soil such that of Joshimath area, determination of void ratio, porosity and permeability characteristics throw an important light on the nature and behaviour of the soil in dry and saturated conditions which in turn govern the internal stability between the different grain sizes within the soil. The void ratio is defined as the ratio of the volume of voids to the volume of the solid [70] and it generally ranges between 0.3 in compacted or well graded soils (significantly less in rocks) and greater than 2.0 for soft clays or organic soils such as peats. The porosity is the ratio of pore volume to its total volume [70] whereas, the permeability (k) is a measure of the ability of a porous material to allow fluids to pass through it. According to U. S. Bureau of Reclamation, soil is classified as (i) Impervious when k < 10-6 cm/sec, (ii) Semi pervious for k between 10-6 to 10-4 cm/sec and (iii) Pervious when k > 10-4 cm/sec. Void ratio (e) and porosity (n) are both measures of the void volume within the soil [82]. They are defined as:

$$e = Vv / Vs \quad \text{and} \quad n\,\% = Vv / Vt \times 100$$

(Vv is Volume of voids; Vs is Volume of solids, Vt is Total volume)

6.2.7. Atterberg Limits and Moisture content:

The Atterberg limits are a basic measurement of the critical moisture contents of soil where it changes their engineering behavior [70]. These limits include liquid limit (LL), plastic limit (PL) and shrinkage limit (SL) and they define the borderline water contents that separate the different states at which a fine grained soil can exist [83]. The liquid limit is the lower limit of viscous flow, plastic limit is lower limit of plastic state and shrinkage limit is lower limit of volume change [70]. When dried below shrinkage limit, there will be no volume reduction (i.e., shrinkage) with the loss of moisture. The soil becomes unsaturated, losing some water in the voids, while there is no further volume reduction.

6.2.8. Liquid Limit (LL)

The liquid limit of a soil is the water content, expressed as percentage of the weight of the oven dried soil, at the boundary between the liquid and plastic states of consistency of the soil [84]. LI is a measure of where the current water content (w) lies with respect to the PL-LL range. The natural water content lying to the right of this range implies LI greater than 1 while to the left of this range, LI is negative. The soils behave as brittle solid below SL, semi-solid between SL and PL, plastic solid between PL and LL and Liquid state above LL (Fig. 9). In addition, plasticity index and shrinkage ratio are also calculated from Atterberg limits.

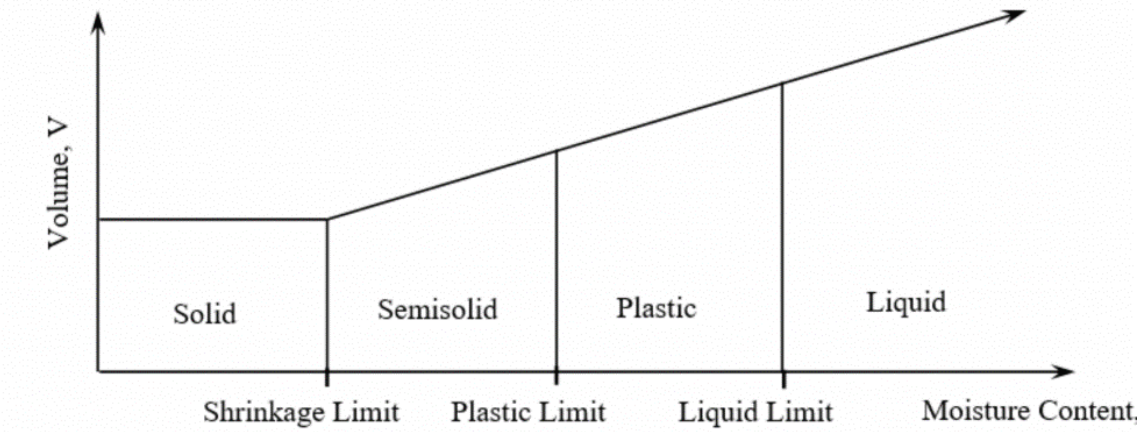

Fig. 9. Graph showing qualitative positions of Atterberg limits on moisture content scale and behavior of soil.

6.2.9. Plastic Limit (PL):

Plastic limit is defined as the lowest water content at which the fine grained soil can be rolled into a 3 mm diameter thread [85, 86, 87]. The soil remains plastic when the water content lies between LL and PL, and the difference between LL and PL is known as the plasticity index (PI).

International Journal of Engineering Research & Technology (IJERT)
ISSN: 2278-0181
Vol. 14 Issue 03, March-2025

6.2.10. Shrinkage Ratio

The shrinkage ratio (SR) is defined as a ratio of decrease in volume of soil expressed as percentage of its dry volume to the corresponding change in its water content above shrinkage limit [82], and it is expressed as.

$$\text{Shrinkage ratio (SR)} = \{(V_1-V_2/V_{dry})*100\}/(W_1-W_2)$$

Where, V_1= Corresponding volume at W_1 water content, V_2= Corresponding volume at W_2 water content, V_{dry} = Dry volume.

6.2.11. Shrinkage Limit:

The shrinkage limit is the maximum water content expressed as a percentage of oven-dried weight at which any further reduction in water content will not cause a decrease in volume of the soil mass, [88]. The value of shrinkage limit is used for understanding the swelling and shrinkage properties of cohesive soils [89].

6.2.12. Plasticity Index

Plasticity index is an index property of any soil which is a measure of plasticity of a soil and pure silts are non-plastic, with typical PI value as 0. [90] classified cohesive soils on the basis of plasticity and suggested PI as the single measure of plasticity and it should be seen along with LL when defining plasticity [91].

7. RESULTS:

The geological mapping revealed a total of 182 ground cracks in Joshimath area between Auli and Alaknanda River and out of these, 55 cracks were identified as new (came into existence in year 2023) and 127 as old) developed before 2023. Amongst the 55 new cracks, 39 cracks developed in the month of January, 2023 which were a result of rapid draining of overburden material due to burst of water (600 LPM) and removal of fines (piping phenomenon) whereas 16 cracks developed during monsoon period of year 2023.

An insight into the orientation and displacement associated with these ground cracks shows that the vertical displacement was less than 0.5m in 137 cracks and they are having continuity limited from few centimetres to 2m without any opening. The remaining 45 no. of cracks exhibit vertical ground displacement more than 0.5 m and these were large, continuous linear/ curvilinear ranging in length up to 50 meters with an opening of more than 5 cm. Furthermore, 32% of the cracks are curvilinear and 68% cracks are linear (Figure

Fig) distributed in two linear arrays i.e. 39.01% in NNW-SSE and 37.91% in NNE-SSW directions, respectively with about 23.08% minor bifurcations in between them aligned along WNW (Fig. 10C).

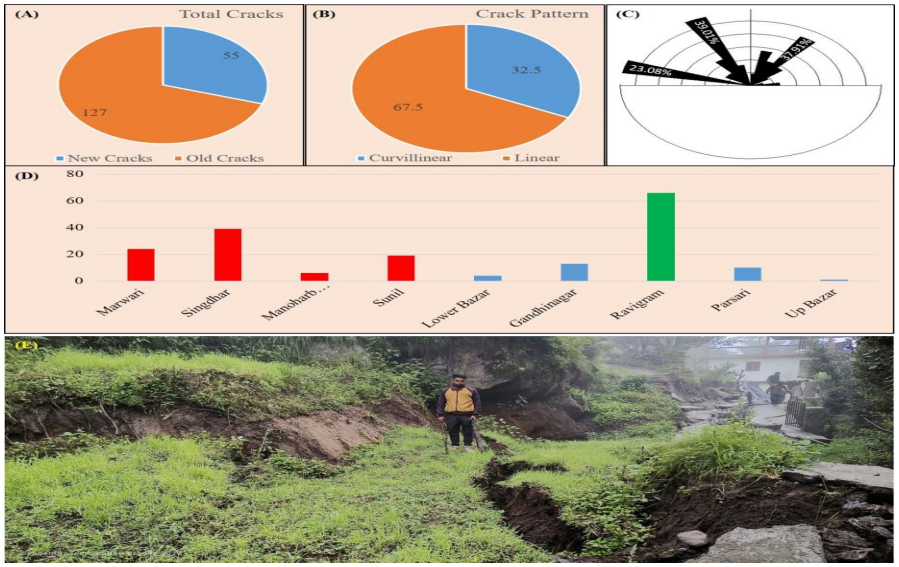

Fig. 10 A) Pie chart showing classification of ground cracks in old and new category; B) Pie chart showing crack pattern classification; C) Rose diagram showing crack orientation vs. crack percentage; D) Bar chart showing distribution of ground cracks; E) newly developed ground crack in Sunil Gaon area

International Journal of Engineering Research & Technology (IJERT)
ISSN: 2278-0181
Vol. 14 Issue 03, March-2025

7.1. Bed Rock Characteristics

The BRS sample collected from Marwadi ward (R-1) is fine to medium-grained granite gneiss with equigranular texture and without any gneissic banding. This sample has lowest density (2.67 gm./cc), lowest water absorption (0.32%), lowest porosity (0.86 %) and has highest void ratio (0.04). The specific gravity of the sample is 2.79 along with lowest Uniaxial Compressive Strength (UCS) value i.e., 178 kgf/cm^2 (Table-4).

The sample collected from the point located west to the Sunil ward (R-5) and from forested area located north of Auli (R-3) is medium to coarse-grained granite gneiss with inequigranular texture and without gneiss banding. These samples have moderate density (2.70-2.74 gm./cc), moderate water absorption (0.35-0.39%) and moderate porosity (0.94-1.05%). The specific gravity of the samples varies between 2.76-2.79; void ratio is 0.01-0.03 and moderate UCS value i.e., 213-233 kgf/cm^2. The samples collected from Ravigram ward from AT nala (R-2) and from Sunil ward (R-4) are coarse to very coarse-grained granite gneiss with well-developed gneissic banding. These samples have highest density (2.83-3.05 gm./cc), highest water absorption (0.43-0.47%), highest porosity (1.30-1.32%), highest specific gravity (2.86-3.08) and low void ratio (0.01). These samples also have the highest UCS value i.e., 305-337 kgf/cm^2.

Table -4: Geotechnical parameters of rock samples (UCS empirically calculated through point load index).

Sample No.	Density (gm/cc)	Water absorption (%)	Specific gravity	Porosity (%)	Void Ratio	Point Load Index (kgf/cm^2)	UCS (kgf/cm^2)
R-1	2.67	0.32	2.79	0.86	0.04	8.07	178
R-2	2.83	0.47	2.86	1.32	0.01	13.87	305
R-3	2.7	0.39	2.79	1.05	0.03	9.69	213
R-4	3.05	0.43	3.08	1.3	0.01	15.3	337
R-5	2.74	0.35	2.76	0.94	0.01	10.58	233

The determined UCS values show positive correlation with the specific gravity, density, porosity and water absorption of the rock mass (Fig. 11). Whereas, the UCS values show negative correlation with the void ratio of the rocks mass (Fig. 11). The calculated correlation coefficient of UCS with other geotechnical parameters also show similar relationship (Fig. 11) with positive correlation values between 0.83-0.94 and -0.82 value of negative correlation with void ratio. The bed rock did not have any role in any type of ground distress features of pattern1,2 or 3 cracks in the study area.

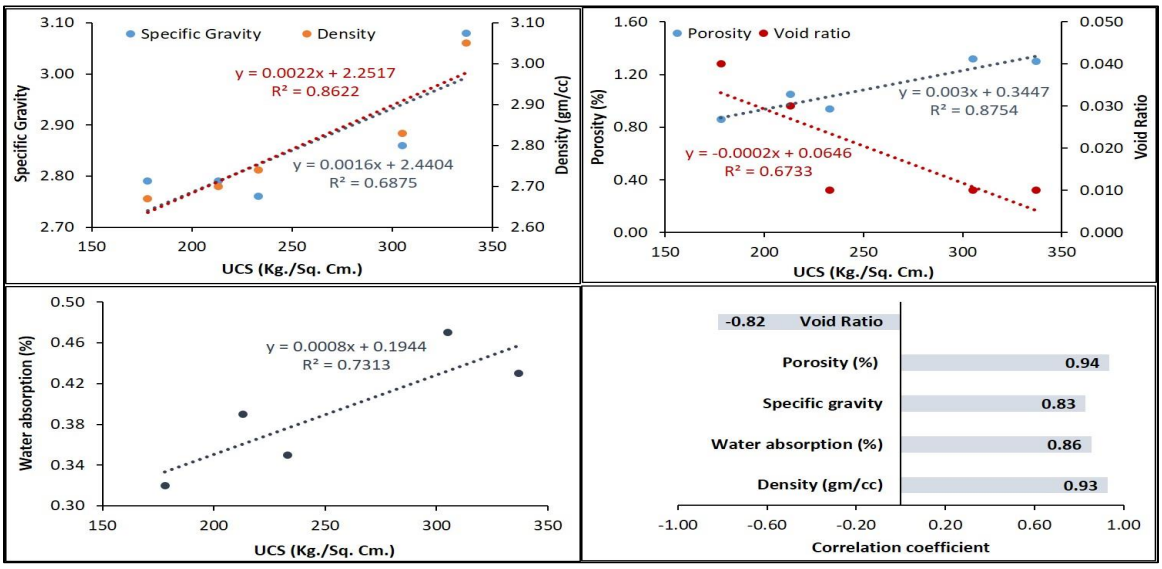

Fig. 11. Correlation of UCS with different geotechnical parameters of bedrock

International Journal of Engineering Research & Technology (IJERT)
ISSN: 2278-0181
Vol. 14 Issue 03, March-2025

7.2. Coarse-grained sandy Soil: Out of total 45 samples collected from different parts of Joshimath, 28 have been found to be coarse-grained sandy matrix as more than 50% material is retained in No. 200 sieve size and pass more than 50% material in no 4-sieve size. All these samples pass more than 12% material in No. 200 sieve size and therefore classified as sands with appreciable amount of fine. Only the sample no-JSS09 falls in the SM-SC class while the remaining 27 nos. of the samples are non-plastic in nature and have been categorized under SM class as per Cassgrande′s plasticity chart for [70] (Fig. 12).

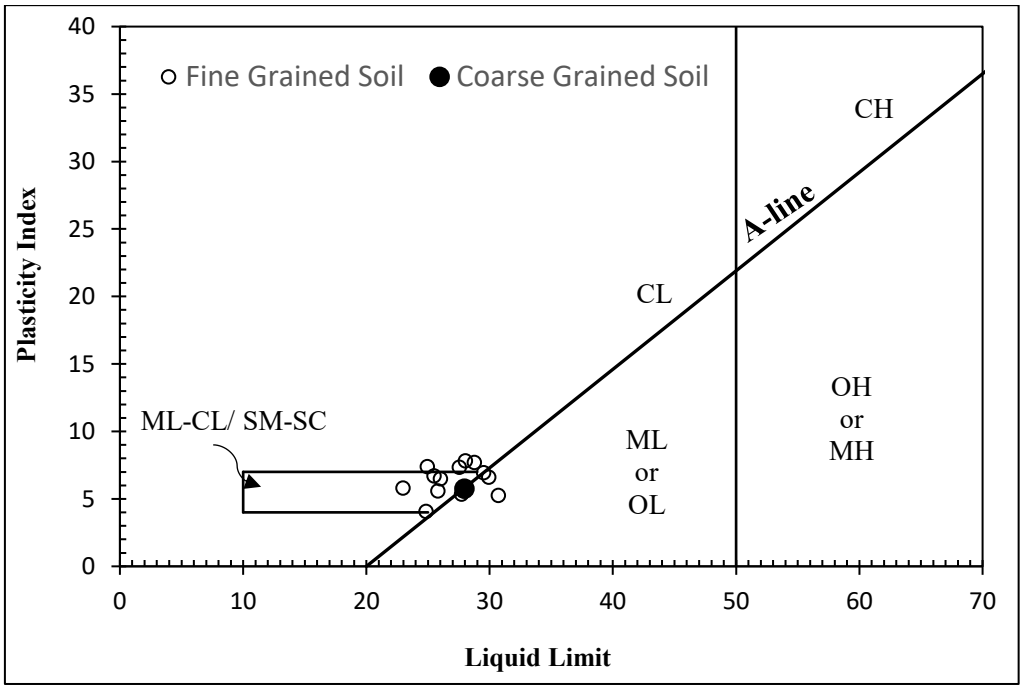

Fig. 12. Casagrande's plasticity chart showing several representative soil types (developed from Casagrande, [91] and [92]) which have been used to define classes of matrix of SFM material from study area.

Grain size distribution curve (Fig. 13) was prepared to understand the grading within individual samples under various types such as well-graded, gap-graded and uniform types. The well-graded soil has a good representation of particle sizes over a wide range and its gradation curve is smooth and generally concave upward whereas, gap-graded matrix is a poorly graded material where there is either an excess or deficiency of certain grain sizes. The matrix of any soil, which consists of particles of same size, is considered to be uniform and hence are poorly graded. The visual estimation of grain size distribution curve of SM matrix suggests dominantly gap-graded character of the soil as the curve covers large fraction of grain sizes. Some of the samples show well graded character with nearly smooth curve (Fig. 13). This variation is also reflected by the variable proportion of gravels (0- 36.9%), sand (33.78 - 84.33%) and silt and clay (13.74 -49.67%) in different samples of SM class and it is also reflected by coefficient of curvature (C_c) and coefficient of uniformity (C_u) (Fig. 14). The other 22 no. of soil samples were classified as poorly graded and remaining 05 no. of soil samples well graded based on C_c and C_u values. The field observations indicate that slopes in Joshimath Township area and Parsari areas are occupied with SM and SM-SC types of soil with scattered clay-rich pockets in between. Furthermore, the distribution of ground cracks indicates that the most of the cracks over these soils are smaller slips on the free faces of slope. The poorly graded nature of the SM-SC matrix is also reflected by coefficient of curvature (Cc) and coefficient of uniformity (Cu) values given in Table 6.

Published by :
http://www.ijert.org

International Journal of Engineering Research & Technology (IJERT)
ISSN: 2278-0181
Vol. 14 Issue 03, March-2025

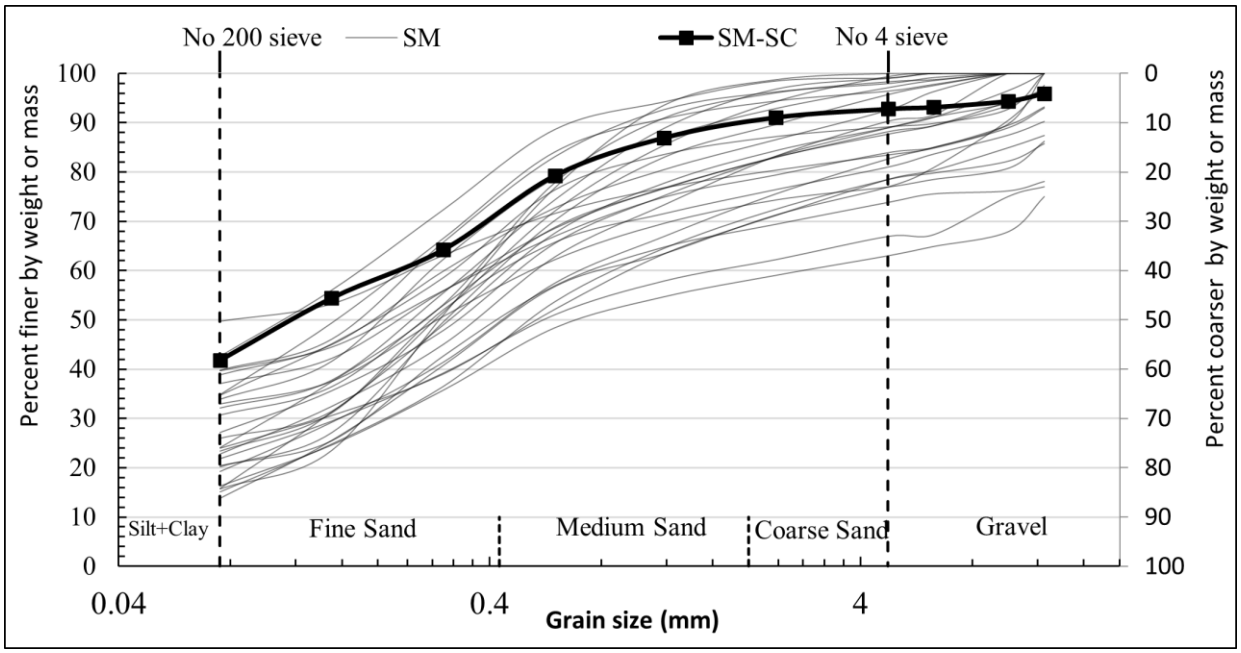

Fig. 13. Grain size distribution curve for different symbol group of coarse-grained sandy matrix.

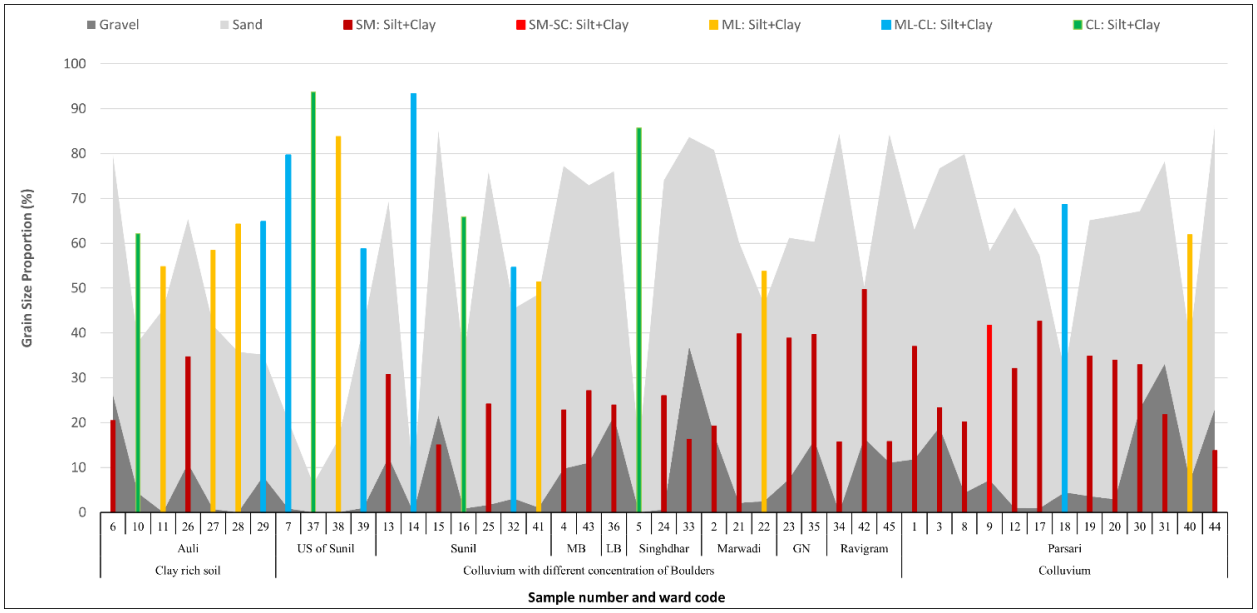

Fig. 14, Graph showing sample wise variation in gravel, sand and silt+clay proportions along with ward code (US of Sunil: Upper slope of Sunil ward; MB: Manoharbagh ward; LB: Lower Bazar ward; GN: Gandhinagar ward, SM: Silt+Clay: Silt+Clay proportion of SM class; SM-SC: Silt+Clay: Silt+Clay proportion of SM-SC class; ML: Silt+Clay: Silt+Clay proportion of ML class; ML-CL: Silt+Clay proportion of ML-CL class; CL: Silt+Clay: Silt+Clay proportion of CL class)

Published by :
http://www.ijert.org

International Journal of Engineering Research & Technology (IJERT)
ISSN: 2278-0181
Vol. 14 Issue 03, March-2025

Table-5: Grain size Analysis, Specific Gravity

Field No.	Sieve opening mm (sample retained on Sieve in %) Sample taken for test- 100 grams											Specific Gravity
	Classification of Soil											
	Gravel				Corse Sand	Medium Sand		Fine Sand		Silt+ Clay		
	12.5	10.0	6.3	4.75	2.36	1.18	0.60	0.30	0.15	0.075	Pan	
JSS-01	3.84	1.95	4.79	1.23	5.25	6.19	8.19	12.74	13.68	5.13	37.01	2.69
JSS-02	0.00	10.28	4.75	2.34	7.11	8.62	9.44	16.04	12.19	9.99	19.24	2.70
JSS-03	9.79	2.75	3.84	2.63	4.59	4.87	5.79	13.70	20.94	7.75	23.35	2.70
JSS-04	0.00	0.00	8.45	1.28	7.12	9.86	10.51	17.75	12.57	9.67	22.79	2.66
JSS-05	0.00	0.00	0.00	0.00	1.53	2.62	2.27	2.16	1.25	4.48	85.69	2.60
JSS-06	21.97	1.90	0.61	1.71	4.46	4.63	7.78	14.28	17.18	5.06	20.42	2.66
JSS-07	0.00	0.00	0.00	0.86	1.17	1.80	2.66	5.58	3.35	4.98	79.60	2.56
JSS-08	0.00	0.00	2.46	1.82	6.10	6.64	12.79	20.63	22.49	6.95	20.12	2.65
JSS-09	4.06	1.54	1.25	0.37	1.71	4.13	7.66	15.07	9.83	12.64	41.74	2.58
JSS-10	0.00	0.00	3.22	1.06	2.11	3.08	4.80	7.94	11.44	4.24	62.11	2.59
JSS-11	0.00	0.00	0.00	0.00	2.05	3.39	6.14	12.29	10.38	10.99	54.76	2.62
JSS-12	0.00	0.00	0.00	1.00	2.19	7.94	14.48	18.91	17.73	5.66	32.09	2.66
JSS-13	3.40	3.16	4.08	1.68	4.64	6.40	7.83	15.82	16.51	5.74	30.74	2.68
JSS-14	0.00	0.00	0.00	0.00	0.10	0.19	0.53	1.20	1.86	2.86	93.26	2.58
JSS-15	14.32	3.55	2.41	1.30	6.06	7.91	10.80	17.20	11.70	9.71	15.04	2.65
JSS-16	0.00	0.00	0.00	0.82	1.41	3.03	4.90	8.67	11.36	3.88	65.93	2.64
JSS-17	0.00	0.00	0.00	0.93	0.62	4.23	5.57	16.29	16.30	13.41	42.65	2.67
JSS-18	3.17	0.00	0.70	0.60	1.58	2.67	3.39	6.79	8.80	3.71	68.59	2.66
JSS-19	0.00	0.00	2.26	1.35	2.02	3.58	6.71	17.53	17.16	14.54	34.85	2.63
JSS-20	0.00	0.00	1.49	1.43	4.23	5.79	8.30	16.45	20.68	7.71	33.92	2.72
JSS-21	0.00	0.00	0.86	1.21	1.70	3.58	9.53	17.35	19.67	6.29	39.81	2.73
JSS-22	0.00	0.00	1.97	0.51	1.45	3.49	7.26	13.25	9.91	8.43	53.73	2.71
JSS-23	0.00	0.00	3.72	3.74	6.02	6.07	7.73	12.85	14.90	6.14	38.83	2.69
JSS-24	0.00	0.00	0.00	0.60	5.06	8.86	13.31	20.54	20.12	5.49	26.02	2.64
JSS-25	0.00	0.00	1.23	0.43	2.24	5.11	13.08	24.74	15.68	13.37	24.12	2.64
JSS-26	0.00	7.29	2.90	0.69	1.98	3.63	7.15	17.82	13.45	10.42	34.67	2.64
JSS-27	0.00	0.00	0.00	0.71	0.36	2.01	4.58	10.49	16.91	6.52	58.42	2.62
JSS-28	0.00	0.00	0.00	0.00	1.00	1.89	4.20	9.33	12.77	6.55	64.26	2.59
JSS-29	4.34	0.00	2.94	0.77	3.26	3.13	4.03	7.56	4.79	4.37	64.81	2.66
JSS-30	13.82	5.47	2.26	1.53	2.64	4.74	7.34	11.53	13.19	4.59	32.89	2.55
JSS-31	23.05	1.97	7.74	0.36	4.72	4.33	6.82	11.85	9.76	7.62	21.78	2.64
JSS-32	0.00	0.00	2.76	0.26	0.45	3.88	6.52	11.23	13.79	6.53	54.58	2.67
JDSS-01	25.01	7.10	3.00	1.87	3.99	4.34	6.26	12.66	11.14	8.31	16.32	2.71
JDSS-02	0.00	0.00	0.00	0.00	1.26	5.17	16.72	25.83	27.52	7.83	15.67	2.70
JDSS-03	6.85	3.70	4.50	1.05	4.54	4.49	7.90	11.04	11.45	4.80	39.68	2.70
JDSS-04	12.56	2.47	4.61	1.82	7.34	7.80	11.22	13.16	8.43	6.64	23.95	2.72
JDSS-05	0.00	0.00	0.00	0.00	0.00	0.33	0.74	1.68	1.58	1.96	93.71	2.59
JDSS-06	0.00	0.00	0.00	0.00	0.58	1.03	1.91	4.70	3.77	4.28	83.77	2.61
JDSS-07	0.00	0.00	0.00	0.98	1.46	4.02	6.90	11.38	12.61	3.93	58.72	2.64

International Journal of Engineering Research & Technology (IJERT)
ISSN: 2278-0181
Vol. 14 Issue 03, March-2025

JDSS-08	0.00	3.91	2.41	0.67	1.30	2.34	4.46	9.67	7.73	5.64	61.87	2.70
JDSS-09	0.00	0.00	0.00	1.05	2.69	4.20	6.78	10.26	16.94	6.75	51.33	2.72
JDSS-10	7.05	3.98	4.14	1.38	3.11	3.57	5.19	8.50	9.87	3.54	49.67	2.46
JDSS-11	3.15	2.89	2.82	2.19	5.80	7.97	9.65	17.71	12.25	8.48	27.09	2.68
JDSS-12	2.49	7.07	9.58	3.92	5.73	7.84	6.64	16.02	15.23	11.74	13.74	2.72
JDSS-13	0	3.52	5.41	2.10	4.69	6.60	10.09	18.65	17.70	15.49	15.75	2.73

Table –6: Moisture Content, Density (Dry & Wet), Porosity, Atterberg's Limit, Direct Shear, Permeability Tests

Field No.	Moisture Content %	Wet Density Gms/cc	Dry Density Gms/cc	Porosity %	Void Ratio	Atterberg's Limit					Direct Shear Test		Permeability Test Cm/sec
						Liquid Limit	Plastic Limit	Shrinkage Limit	Shrinkage Ratio	Plastic Index	'C' (Kpa)	'Ø' degree	
JSS-01	9.53	1.93	1.76	0.35	0.53	Non Plastic Soil					7.50	44.9	Non Plastic Soil
JSS-02	11.58	1.96	1.76	0.35	0.53	Non Plastic Soil					5.00	38.1	Non Plastic Soil
JSS-03	12.74	2.05	1.82	0.33	0.70	Non Plastic Soil					7.50	42.3	Non Plastic Soil
JSS-04	11.99	1.98	1.77	0.34	0.71	Non Plastic Soil					5.00	39.8	Non Plastic Soil
JSS-05	16.26	1.81	1.56	0.40	0.67	27.56	20.22	15.47	1.86	7.34	20.00	32.6	0.00000169
JSS-06	22.00	1.89	1.55	0.42	0.85	Non Plastic Soil					2.50	46.8	Non Plastic Soil
JSS-07	18.63	2.05	1.73	0.32	0.48	29.52	22.59	18.89	1.76	6.93	22.50	37.8	0.00000188
JSS-08	12.97	1.85	1.64	0.38	0.62	Non Plastic Soil					5.00	40.1	Non Plastic Soil
JSS-09	20.44	1.87	1.55	0.40	0.67	27.97	22.22	18.26	1.78	5.75	22.50	33.0	0.00000313
JSS-10	30.76	1.81	1.38	0.47	0.88	28.78	21.08	18.05	1.75	7.70	27.50	37.1	0.000000978
JSS-11	23.60	1.52	1.23	0.53	1.13	30.71	25.46	21.45	1.67	5.25	22.60	36.0	0.00000783
JSS-12	13.36	1.89	1.67	0.37	0.59	Non Plastic Soil					7.50	42.3	Non Plastic Soil
JSS-13	14.45	1.87	1.63	0..9	0.64	Non Plastic Soil					7.50	43.2	Non Plastic Soil
JSS-14	18.58	1.89	1.59	0.38	0.62	26.02	19.52	16.44	1.79	6.50	22.50	39.5	0.000000927
JSS-15	16.86	1.88	1.61	0.39	0.65	Non Plastic Soil					7.50	40.8	Non Plastic Soil
JSS-16	15.12	2.01	1.75	0.34	0.51	24.96					17.58	15.54	1.87
JSS-17	16.93	1.97	1.68	0.37	0.59	Non Plastic Soil					7.50	42.3	Non Plastic Soil
JSS-18	15.71	2.01	1.74	0.35	0.52	25.49					18.78	15.45	1.89
JSS-19	24.18	1.72	1.39	0.47	0.89	Non Plastic Soil					0.00	40.1	Non Plastic Soil
JSS-20	16.96	1.79	1.53	0.44	0.78	Non Plastic Soil					2.50	40.1	Non Plastic Soil
JSS-21	16.90	1.81	1.55	0.43	0.76	Non Plastic Soil					10.00	40.5	Non Plastic Soil
JSS-22	15.74	1.87	1.62	0.40	0.67	Non Plastic Soil					7.50	43.5	Non Plastic Soil
JSS-23	10.18	1.78	1.62	0.40	0.66	Non Plastic Soil					7.50	41.1	Non Plastic Soil
JSS-24	9.24	1.84	1.68	0.36	0.57	Non Plastic Soil					5.00	42.0	Non Plastic Soil
JSS-25	15.33	1.90	1.65	0.38	0.60	Non Plastic Soil					7.50	42.0	Non Plastic Soil
JSS-26	29.82	1.84	1.42	0.46	0.86	Non Plastic Soil					7.50	43.8	Non Plastic Soil
JSS-27	19.07	1.86	1.56	0.41	0.68	Non Plastic Soil					7.50	43.2	Non Plastic Soil
JSS-28	27.89	1.68	1.31	0.49	0.98	27.73					22.37	19.53	1.74
JSS-29	21.69	1.90	1.56	0.41	0.71	25.80					20.22	17.09	1.83

International Journal of Engineering Research & Technology (IJERT)
ISSN: 2278-0181
Vol. 14 Issue 03, March-2025

JSS-30	19.61	1.52	1.27	0.51	1.01	Non Plastic Soil	7.50	41.1	Non Plastic Soil
JSS-31	18.22	1.63	1.38	0.48	0.91	Non Plastic Soil	7.50	40.8	Non Plastic Soil
JSS-32	17.61	1.91	1.62	0.39	0.65	22.99	17.18	16.61	1.84
JDSS-01	Disturbed samples						7.50	41.4	
JDSS-02						Non Plastic Soil	7.50	40.1	Non Plastic Soil
JDSS-03						Non Plastic Soil	5.00	43.2	Non Plastic Soil
JDSS-04						Non Plastic Soil	5.00	44.4	Non Plastic Soil
JDSS-05						Non Plastic Soil	20.22	16.50	Non Plastic Soil
JDSS-06						28.04	23.33	19.22	1.84
JDSS-07						29.95	20.76	19.34	1.78
JDSS-08						24.84	10	40.8	1.77
JDSS-09						Non Plastic Soil	7.50	42.0	Non Plastic Soil
JDSS-10						Non Plastic Soil	7.50	43.5	Non Plastic Soil
JDSS-11						Non Plastic Soil	5.00	41.1	Non Plastic Soil
JDSS-12						Non Plastic Soil	5.00	42.9	Non Plastic Soil
JDSS-13						Non Plastic Soil	5.00	39.5	Non Plastic Soil
						Non Plastic Soil			Non Plastic Soil

Table -7: Table showing matrix classification based on Unified Soil Classification System and geotechnical parameters.

Sample No	Grain size	USCS Class	Coefficient of Uniformity (Cu)	Coefficient of Curvature (Cc)	Gradin g	Plasticity	Permeability (Cm/Sec)	Cohesion (Kpa)	State
1	Coarse grained	SM	16.66	0.40	Poor	None	Pervious	Very soft	-
2	Coarse grained	SM	0.60	24.57	Poor	None	Pervious	Very soft	-
3	Coarse grained	SM	13.56	1.17	Well	None	Pervious	Very soft	-
4	Coarse grained	SM	15.48	0.87	Poor	None	Pervious	Very soft	-
5	Fine grained	CL	4.10	1.22	Well	Low	Semi Pervious	Very soft	Semi Solid
6	Coarse grained	SM	21.08	1.10	Well	None	Pervious	Very soft	-
7	Fine grained	ML-CL	4.19	1.24	Well	Low	Semi Pervious	Very soft	Solid
8	Coarse grained	SM	11.35	1.60	Well	None	Pervious	Very soft	-
9	Coarse grained	SM-SC	10.83	0.60	Poor	Low	Semi Pervious	Very soft	Semi Solid
10	Fine grained	CL	4.46	1.27	Well	Low	Impervious	Soft	Liquid
11	Fine grained	ML	6.23	0.95	Poor	Low	Semi Pervious	Very soft	Semi Solid
12	Coarse	SM	13.86	0.50	Poor	None	Pervious	Very soft	-

International Journal of Engineering Research & Technology (IJERT)
ISSN: 2278-0181
Vol. 14 Issue 03, March-2025

	grained								
13	Coarse grained	SM	15.59	0.45	Poor	None	Pervious	Very soft	-
14	Fine grained	ML-CL	4.00	1.21	Well	Low	Impervious	Very soft	Semi Solid
15	Coarse grained	SM	18.26	0.97	Poor	None	Pervious	Very soft	-
16	Fine grained	CL	4.40	1.27	Well	Low	Impervious	Soft	Solid
17	Coarse grained	SM	8.70	0.74	Poor	None	Pervious	Very soft	-
18	Fine grained	ML-CL	4.36	1.26	Well	Low	Semi Pervious	Soft	Semi Solid
19	Coarse grained	SM	9.68	0.70	Poor	None	Pervious	Very soft	-
20	Coarse grained	SM	11.05	0.62	Poor	None	Pervious	Very soft	-
21	Coarse grained	SM	11.34	0.58	Poor	None	Pervious	Very soft	-
22	Fine grained	ML	7.25	0.82	Poor	None	Pervious	Very soft	-
23	Coarse grained	SM	13.16	0.50	Poor	None	Pervious	Very soft	-
24	Coarse grained	SM	13.24	1.24	Well	None	Pervious	Very soft	-
25	Coarse grained	SM	11.25	0.90	Poor	None	Pervious	Very soft	-
26	Coarse grained	SM	12.89	0.53	Poor	None	Pervious	Very soft	-
27	Fine grained	ML	5.49	1.06	Well	None	Pervious	Very soft	-
28	Fine grained	ML	4.43	1.27	Well	Low	Semi Pervious	Very soft	Liquid
29	Fine grained	ML-CL	4.42	1.27	Well	Low	Semi Pervious	Very soft	Plastic
30	Coarse grained	SM	20.65	0.33	Poor	None	Pervious	Very soft	-
31	Coarse grained	SM	47.69	0.39	Poor	None	Pervious	Very soft	-
32	Fine grained	ML-CL	7.70	0.77	Poor	Low	Pervious	Soft	Plastic
33	Coarse grained	SM	61.41	0.35	Poor	None	Pervious	Very soft	-
34	Coarse grained	SM	8.14	1.71	Well	None	Pervious	Very soft	-
35	Coarse grained	SM	18.14	0.36	Poor	None	Pervious	Very soft	-
36	Coarse grained	SM	29.34	0.60	Poor	None	Pervious	Very soft	-

International Journal of Engineering Research & Technology (IJERT)
ISSN: 2278-0181
Vol. 14 Issue 03, March-2025

37	Fine grained	CL	4.00	1.21	Well	Low	Semi Pervious	Soft	-
38	Fine grained	ML	4.13	1.23	Well	Low	Semi Pervious	Very soft	-
39	Fine grained	ML-CL	5.88	0.99	Poor	Slight	Semi Pervious	Very soft	-
40	Fine grained	ML	4.47	1.28	Well	None	Pervious	Very soft	-
41	Fine grained	ML	8.96	0.68	Poor	None	Pervious	Very soft	-
42	Coarse grained	SM	13.26	0.46	Poor	None	Pervious	Very soft	-
43	Coarse grained	SM	16.42	0.44	Poor	None	Pervious	Very soft	-
44	Coarse grained	SM	15.83	0.76	Poor	None	Pervious	Very soft	-
45	Coarse grained	SM	9.67	0.88	Poor	None	Pervious	Very soft	-

7.3. Fine-grained silt and clayey Soil: The analysis of soil samples also revealed that in 17 soil samples more than 50% material pass through No. 200 sieve size which categorizes them under fine-grained silt and clayey soil (Table-8). The grain size distribution curve of fine-grained silt and clayey matrix suggests dominantly well graded nature of the material, (Fig. 15) whereas, some of the samples show gap graded nature. There are variable proportions of gravels, sand and silt+clay in the fine-grained matrix and the CL class soil has 0 - 4.28% gravels, 6.29 - 33.61% sand and 62.11 - 93.71% silt and clay proportions. The ML-CL class soil on the other hand has 0-8.05% gravels, 6.74 - 42.4% sand and 54.58 - 93.26% silt and clay proportions. The ML class matrix has 0 - 6.99% gravels, 16.27 - 47.62% sand and 51.33 - 83.77% silt and clay proportions.

Published by :
http://www.ijert.org

International Journal of Engineering Research & Technology (IJERT)
ISSN: 2278-0181
Vol. 14 Issue 03, March-2025

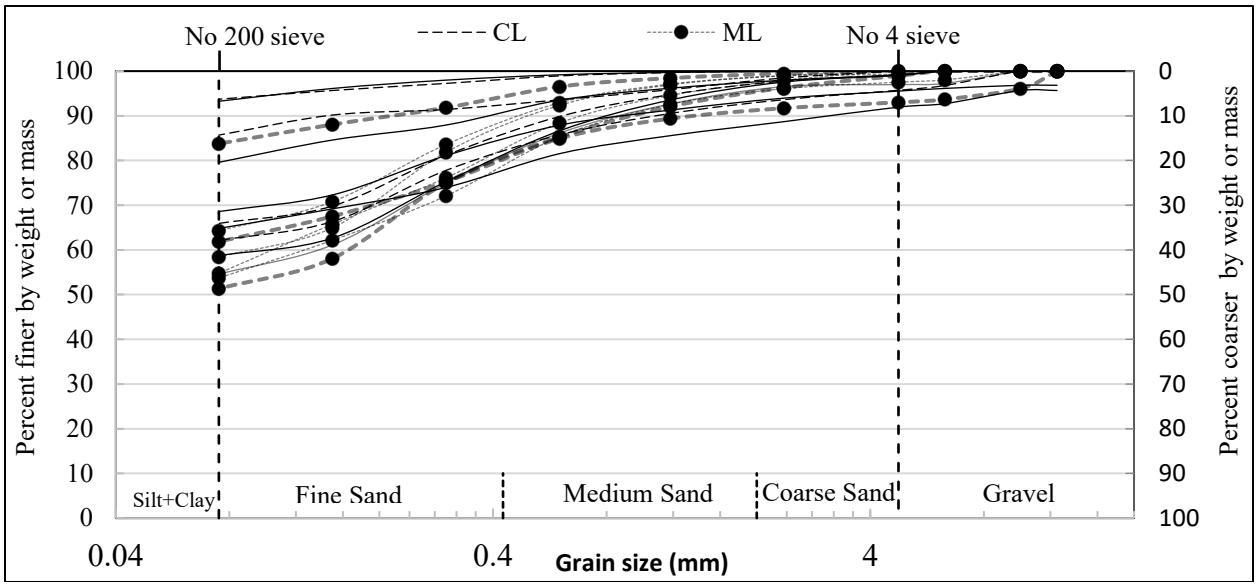

Fig. 15 Grain distribution curve for different classes of fine-grained matrix.

Out of total 17 nos. of fine-grained matrix samples, 12 no. of samples are well graded and 05 no. samples are poorly graded based on C_c and C_u values while all the four samples of CL class are well graded based on C_c and C_u values (table 7). The seven samples were classified as ML class of which four samples were well graded and three as poorly graded whereas out of the six samples classified as ML-CL class, four samples were well graded and two were poorly graded.

Table -8: Table showing classification of matrix samples based on USCS scheme.

Major Divisions	Group Symbols	No. of samples	Typical Names	
Coarse grained sandy matrix (28 no of samples)	SM	27	Silty sands, sand silt mixtures	
	SM-SC	01	SM: Silty sands, sand silt mixtures SC: Clayey sands, sand-clay mixtures	Silty sand with minor clay
Fine grained silt and clayey matrix (17 no of samples)	ML	07	Inorganic silts and very fine sands, Silty or clayey fine sands or clayey silts	
	CL	04	Sandy clays, silty clays, lean clays	
	ML-CL	06	Silty or clayey fine sands or clayey silts	

These results of our study were compared with the Grain Size Distribution (GSD) analysis carried out by Indian Institute of Technology Roorkee [40] which also indicated that the soils from Joshimath hill slope are predominantly Gravelly Sands with boulders. Further, the Dynamic Cone Penetration Test (DCPT) tests by IIT Roorkee, showed high degree of variability indicating the heterogeneity in the sub-surface strata wherein very high values of refusal of the cone penetration were observed where large boulders were encountered below the surface, however, there was a sudden drop in the DCPT value which indicated presence of loose soil deposits underneath the gravels and boulders [40]. MASW survey [40] shows a dispersion image with a very high scatter which clearly indicates a complex mix

Published by :
http://www.ijert.org

International Journal of Engineering Research & Technology (IJERT)
ISSN: 2278-0181
Vol. 14 Issue 03, March-2025

of variable size particles of soil and it also predicted that the same heterogeneous mass continues to greater depths below the surface [40].

Authors have further compared their results with the outcomes of the geophysical studies carried out by National Geophysical Research Institute (NGRI) through Electric Vector Resistivity Survey (EVRI), Multichannel Analysis of Shear Waves (MASW) and Ground Penetration Radar (GPR) to decipher the configuration of overburden material/soil over Joshimath hill slope, the subsurface flow and its channelization obstruction [41]. The EVRI survey reflected that the thick ness of overburden in the Joshimath hill slope is different in different parts and where it was

> 50 m around Manoharbagh and Narsingh Temple areas while in the lower part of the hill slope i.e. below Marwadi area it was shallow [41]. The ground fissures are mostly present in the areas with thick overburden cover but subsidence fissures also affect the margin areas [4].

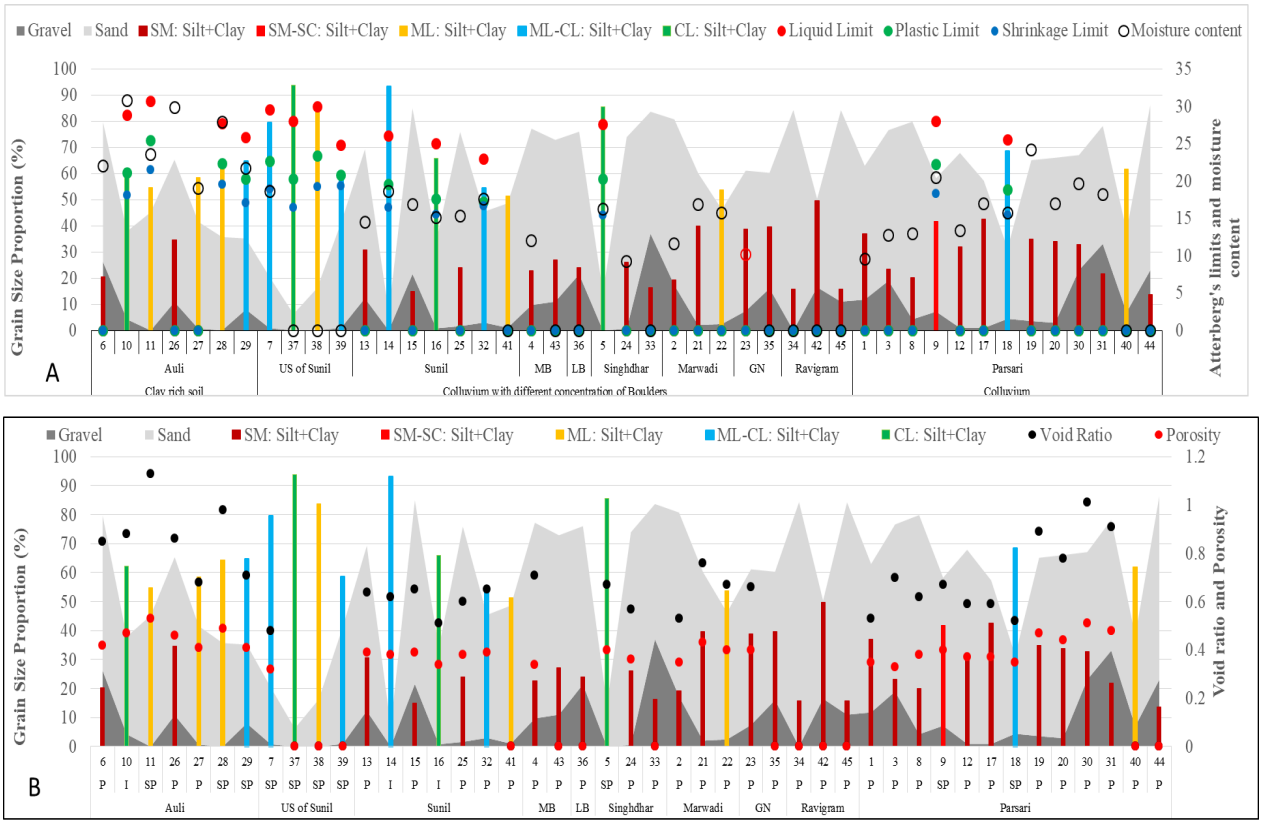

Fig.16: A) Graph showing variation in proportions of gravel, sand and silt+clay along with liquid limit, plastic limit, shrinkage ratio and moisture content of different matrix types. (Area code: US of Sunil: Upper slope of Sunil ward; MB: Manoharbagh ward; LB: Lower Bazar ward; GN: Gandhinagar ward; SM: Silt+Clay: Silt+Clay proportion of SM class; SM-SC: Silt+Clay: Silt+Clay proportion of SM-SC class; ML: Silt+Clay: Silt+Clay proportion of ML class; ML-CL: Silt+Clay proportion of ML-CL class; CL: Silt+Clay: Silt+Clay proportion of CL class). B)variation in void ratio, porosity and permeability class with respect to different matrix classes along with varying proportion of gravel, sand and silt+clay (Permeability class code: P: Pervious; SP: Semi-pervious; I: Impervious).

International Journal of Engineering Research & Technology (IJERT)
ISSN: 2278-0181
Vol. 14 Issue 03, March-2025

The results of Atterburg limit tests indicate that 31 samples collected from the study area are non-plastic and remaining 14 samples are plastic in character. The disturbed samples does not have moisture content and hence for them only the Atterberg limits are plotted against grain size classes whereas the non-plastic samples do not have any Atterberg limits and in their case moisture content has been plotted to visualize the variation (Fig 16A). The plastic fine-grained silt samples with clay rich matrix of CL, ML & ML-CL classes have moisture content greater than its shrinkage limit or at the margin whereas some of the samples have moisture content greater than plastic limit and/or liquid limit. The liquid limit of SM-SC class is 27.97% and therefore the liquid limit of SM class is expected to be lower than this. As such, the liquid limit of non-plastic sandy soil is considered to be <20%.
The Grain Size Distribution (GSD) analysis by IIT – R also confirms that the predominantly Gravelly Sands with boulders lying over Joshimath hill slope are largely non-plastic in nature with a Natural Moisture Content (NMC) ranging between 3% and 25 % [40]. The MASW survey by NGRI shows that the top 5-10m layer of soil is soft-stiff soil characterized by Vs<360m/s which is underlain by 10-20m thick stiff-dense soil with a velocity of >760m/s [41] and it is the former layer which is variously saturated in the middle and lower parts of hill slope around Marwadi, Narsingh Mandir, and Manoharbagh [41]. The GPR survey also brought out that the top layer up to 5m is poorly saturated the saturated layer is 15 - 20 m below the surface which also corroborates with the higher velocity dense soil of MASW [41]. The saturated zones were delineated in Marwadi, Singdhar, Manoharbagh, Sunil, and JP areas [41].
The studies carried out by IITR and NGRI strongly corroborate the conditions of different soils, their saturation and moisture content as brought out by our surface geological and geotechnical studies.

7.4. Classification of Fine-Grained Soils Based on Plasticity

PI and LL are the main parameters used in the classification of fine grained soils including silty clays and clayey silts. The plasticity index range of the soil samples (Table 9) suggests that 31 no. of samples are non-plastic, one sample has slight plasticity and 13 samples have low plasticity. Liquid limit and plasticity index have been used for assessing the swelling potential of soil and according to [94] liquid limit of less than 50% and plasticity index less than 25 indicates low potential of swelling. Since all the analyzed soil samples of study area have liquid limit less than 30.71 and plasticity index less than 7.82, hence it is clearly indicates that the soil in Joshimath area is non-swelling type.

Table -9: Classification of soil samples of Joshimath based on Plasticity Index (PI) categories according to [93].

Matrix Type	No. of samples	PI range	Classification based on Plasticity	Shrinkage Ratio
SM	27	Non-plastic	Non-plastic (PI = 0)	--
ML	04	Non-plastic		--
ML-CL	01	4.08	Slight Plastic (PI = 1 to 5)	1.77
SM-SC	01	5.75	Low Plasticity (PI = 5 to 10)	1.78
ML	03	5.25-6.62		1.67-1.78
ML-CL	05	5.58-6.93		1.76-1.89
CL	04	7.34-7.82		1.75-1.87

7.4.1. Granular Soils

Granular soils have higher permeability than cohesive soils (Table 10) and within granular soils, the permeability increases with the grain size and in general, granular soils are considered to be free draining as long as the presence of fines is less than15 % and fines in excess of 30 % can reduce the permeability significantly.
Table -10: Variation in void ratio, porosity and permeability in different soil classes

International Journal of Engineering Research & Technology (IJERT)
ISSN: 2278-0181
Vol. 14 Issue 03, March-2025

Matrix Type	No. of samples	Void ratio	Porosity (%)	Permeability (Cm./Sec.)	Classification based on permeability
SM	27	0.53-1.01	0.33-0.51	--	Pervious
SM-SC	1	0.67	0.4	$3.13*10^{-6}$	Semi Pervious
ML-CL	1	0.65	0.39	--	Pervious
ML-CL	4	0.48-0.71	0.32-0.41	$1.88*10^{-6}$-$11.3*10^{-6}$	Semi Pervious
ML-CL	1	0.62	0.38	$0.927*10^{-6}$	Impervious
ML	4	0.67-0.68	0.40-0.41	--	Pervious
ML	3	0.98-1.13	0.49-0.53	$3.50*10^{-6}$-$7.83*10^{-6}$	Semi Pervious
CL	2	0.67	0.4	$1.69*10^{-6}$-$4.54*10^{-6}$	Semi Pervious
CL	2	0.51-0.88	0.34-0.47	$0.893*10^{-6}$-$0.978*10^{-6}$	Impervious

The ML soil class (Table- 10) in the study area shows the highest void ratio (1.13) and porosity (0.53) but it is semi pervious while the ML-CL is characterized by lowest void ratio (0.48) and porosity (0.32) although being semi pervious. The SM type non-plastic soils on the other hand are pervious (Table-10) but they exhibit intermediate void ratio and porosity (Fig. 16B). The silt+clay rich soils from Auli area and few samples from Parsari area, have comparatively higher void ratio along with high porosity.

7.4.2. Shear Strength Parameters :The shear resistance of soil is the result of friction and the interlocking of particles and possibly cementation or bonding at the particle contacts. The shear strength parameters of soil samples i.e. cohesion (c) and the angle of internal friction angle (ø) and their variation with respect to grain size of different soil classes are shown in figure 17. The laboratory results of the soil samples from the study area clearly indicate that the higher proportion of silt+clay have higher cohesion values but lower friction angle, whereas, the samples with higher proportion of sand have lower cohesion values but have higher friction angle (Table 11). The CL, ML, ML-CL and SM-SC soil types have higher cohesion values but lower friction angle except a few samples while SM soils have lower cohesion values but have higher friction angle .

Table 11: Shear Parameters of Soil Samples with Grain size classes

Matrix Type	No. of samples	Cohesion (C)	Cohesion based classification	Friction angle (Ø)
SM	27	0-10	Very soft (<24)	38.1-46.8
SM-SC	01	22.5	Very soft (<24)	33
ML-CL	04	12.5-22.5	Very soft (<24)	37.8-42.3
ML-CL	02	25-25	Soft (24 to <48)	34.1-42.3
ML	07	7.5-22.6	Very soft (<24)	36-43.5
CL	01	20	Very soft (<24)	32.6
CL	03	25-27.5	Soft (24 to <48)	33-37.4

The soil samples of study area can be classified in two groups i.e., very soft and soft based on classification of cohesion values of [95]. The spatial distribution of samples suggests that the soil of upper part of hill slope (covering Auli and upper part of Sunil gaon) have good cohesion but the samples from other areas have very low cohesion except a few sporadic samples.
Indian Institute of Technology Roorkee (IIT-R) determined the shear strength characteristics and bearing capacity of soil (Fig. 18) occupying the Joshimath slope at 10 locations through Multi-channel Analysis of Surface Waves (MASW) along with horizontal-to-vertical spectral ratio (HVSR) and through Dynamic Cone Penetration Test (DCPT). The shear parameters derived through DST show the range of cohesion from 0 to 37 kPa and that of angle of internal friction between 14° between 43° respectively. The ultimate and safe load carrying capacities of the soil as determined through Point Load Test [40] are in the range of 8.5 t/m^2 to 44 t/m^2,(Fig. 18) whereas the safe bearing capacity was found ranging between2.8 t/m^2 and 14.67 t/m^2.

Published by :
http://www.ijert.org

International Journal of Engineering Research & Technology (IJERT)
ISSN: 2278-0181
Vol. 14 Issue 03, March-2025

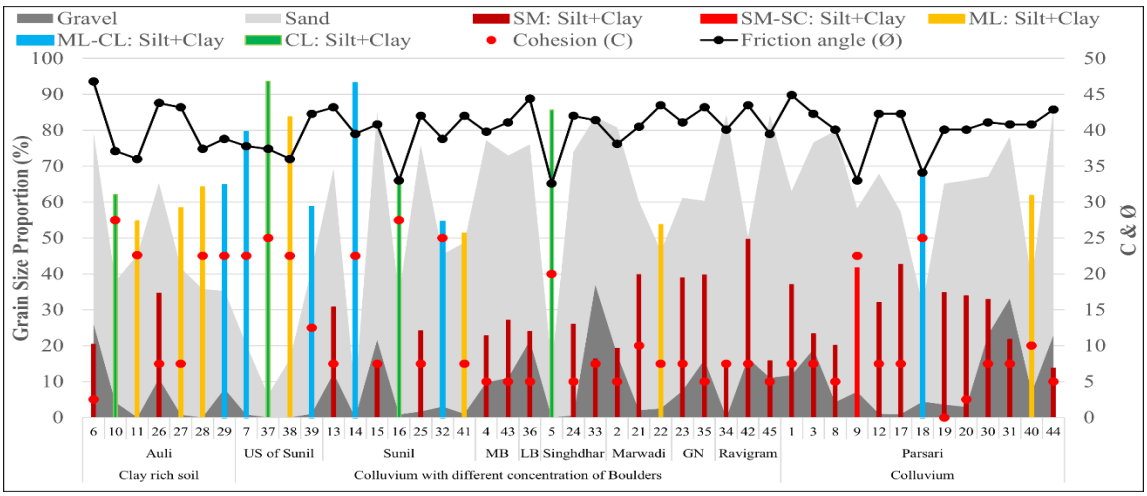

Fig. 17 Graph showing sample wise variation in cohesion and friction angle with respect to different matrix classes along with varying proportion of gravel, sand and silt+clay

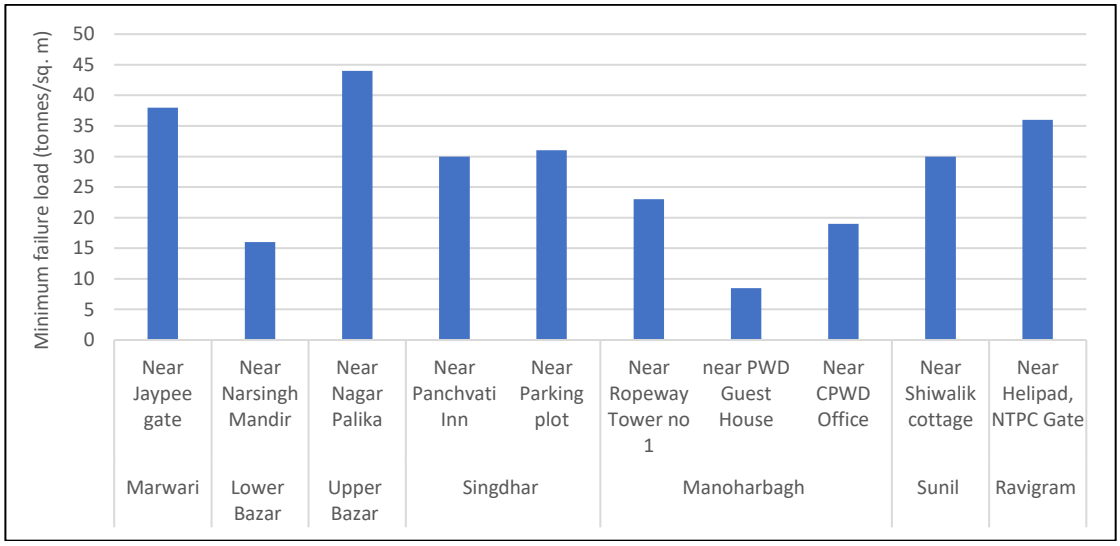

Fig. 18: Locality wise variation in load carrying capacities of the soil [40]

8. Relation between Soil Moisture and Rainfall in the area

In order to find out any relation between the rainfall pattern and the moisture content of the soils in Joshimath area the data on soil volumetric moisture content (VMC) was downloaded from the website of National Weathered Service [96] of USA and rainfall data from [97]. This data represents a pixel of the 9km grid and comes from 05 cm below the surface and shows how much moisture is there in per cubic centimeter volume of the soil. The month wise data was downloaded for the years 2021, 2022, 2023 and 2024 and processed with respect to the upper (sourthern) and lower (northern) parts of Joshimath hill slope. The analysis of the data reveals that the upper and middle hill slope (i.e. southern part) had a higher moisture content than the lower hill slopes (northern part) and it may because of the fact that the upper and middle hill slopes are comparatively gentle and middle slopes in particular have a high thick ness of overburden/soil which allows water to percolate and get stored for a longer duration. The lower parts of the hill slope (northern part) exhibit slightly steep angle of slope and less thickness of soil, which facilitates water to drain out and enter the master stream i.e. Alaknanda River, at the bottom part of the valley. Moreover, a positive corelationship between the rainfall and the variation in the moisture content of the soil is clearly discernible (Fig. 19a, b, c and d) which shows an increase in the moisture content increased with rainfall the increasing and vice versa.

Published by :
http://www.ijert.org

International Journal of Engineering Research & Technology (IJERT)
ISSN: 2278-0181
Vol. 14 Issue 03, March-2025

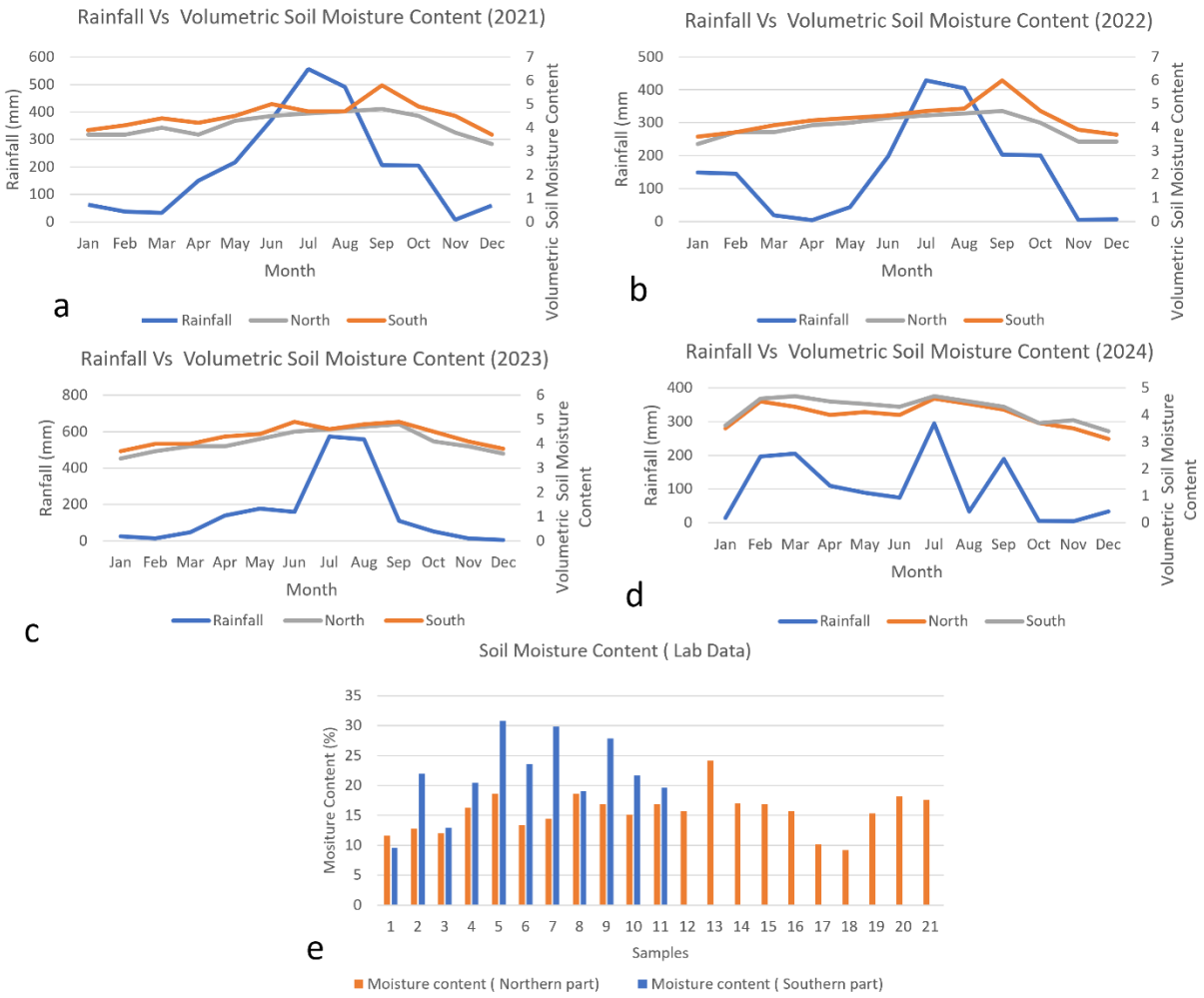

Fig. 19. monthly Volumetric Moisture content (VMC) and rainfall data from Joshimath Town, a) VMC and rainfall data of 2021, b) VMC and rainfall data of 2022, c) VMC and rainfall data of 2023, d) VMC and rainfall data of 2024 , e) plot of laboratory data of soil moisture content from July to August of 2023,

The plot of laboratory data of soil moisture content from July to August of 2023 (Fig. 19e) also shows higher proportion of moisture content in the upper – middle part (southern portion) of the hill slope as compared to the lower (northern portion) of Joshimath hill slope. Further, the plot of moisture content of the soil samples of the study area demonstrates a strong correlation between the rainfall data for the months of July and August 2023 (Fig. 18c).

International Journal of Engineering Research & Technology (IJERT)
ISSN: 2278-0181
Vol. 14 Issue 03, March-2025

Since most of the samples had more than 25% moisture due to increased rainfall, the soil moisture content is classified as wet to very wet. It thus augments the inference that middle part of the hill slope where the overburden thickness is maximum and which is characterized by SM type boulder colluvium, was highly saturated which in turn indicates towards a possibility of high pore water pressure in the soil mass close to the surface, just back of the slope profile, in the middle and middle lower part of the hill slope.

9. DISCUSSIONS:

Geological mapping and profiling along and across the upper middle and lower parts of the hill, slope of Joshimath have clearly brought out the fact that the hill slope is occupied by a thick pile of highly heterogeneous overburden/soil material which varies in thickness from 1 to 4m in the bottommost part and on the flanks of major drainages to more than 100m in the middle part of the hill slope particularly to the west of the geomorphic divide i.e. Singdhar high. The variation in the nature and thickness of the soil has been well corroborated by the geophysical studies carried out by IITR and NGRI through AVRI, DCPT, MASW surveys.

After a careful study and identification, three different patterns have been delineated for the different ground deformations in Joshimath area [11,12]. The Pattern-1 cracks represent the ground subsidence that occurred in the aftermath of the incidence of 2nd January 2023 are a result of sudden draining of the matrix of slope forming material .These NNW-SSE aligned ground cracks are confined to the western side of the geomorphic high (Singdhar high) in the areas around Marwadi-Singdhar-Manoharbagh-Sunil gaon, in the middle part of the hill slope. The Pattern-2 Ground cracks are aligned NNW-SSE to NNE-SSW and are mostly confined to the fringe areas flanking the nala channels (viz. AT nala, Parsari nala) and hence are directly attributable to the process of valley widening along 2nd and 3rd order channels in a dynamically evolving higher Himalayan terrain. Pattern-3 ground cracks, on the other hand, are representatives of the ground cracks which are on the margins of the terraces or load benches are also a result of natural process of sliding along the free face in hilly terrain. It may be mentioned here that the Pattern 2 and Pattern 3 ground cracks pre date the event of burst of water on 2nd January 2023 and hence have no relation with that.

Based on the results of grain size analysis the soil samples of the study have been classified in five different classes i.e., SM, SM-SC, ML, ML-CL & CL. The present study has also identified three major domains i.e., clay dominated soil in Auli area (in the upper hill slope), colluvium with boulders in Joshimath Township area (middle hill slope) and colluvium without or less boulders in Parsari area (western flank of hill slope). The field geotechnical investigations, however, suggests dominance of SM class non plastic soil is the dominant type in the mapped area with intermittent bands of SM-SC, ML, ML-CL & CL class at different elevations. The upper part of the hill slope in Auli area is occupied by clay dominated soil and the same has been classified as clayey SM soil, however, the pockets of these fine-grained soils are also present in the clayey SM soil located east of North-South slope divide in Auli area (Fig. 8).

Overlaying of ground distress features on the slope forming material map (Fig. 8) there appears a direct relation between the pattern 1 ground deformation and SM class bouldery colluvium (Fig. 7). On the other hand the colluvium without or fewer boulders i.e. SM colluvium was largely confined to the western part of upper hill slope around Parsari area (Fig. 8) which was least affected by the ground subsidence but there are incidences of valley slope failures along the nala sections i.e. pattern 2 cracks (Fig. 7a-e).

There is a clear relationship between the pattern 1 ground cracks (developed in the event of 2nd January, 2023) and the dry and wet density of the soil as they are present in the area with high wet density range (1.84-1.93) and high dry density range (1.62-1.71) e.g. in Singdhar, Manoharbagh and Marwadi areas, located in the lower middle part of the hill slope. However, the pattern 2 and 3 cracks in the area have been found to be in the areas having the soil with wide range of dry density (1.40-1.71) and wet density (1.72-1.94) leading to no apparent inference or relations. It thus again proves the finding that occurence of pattern 2 and 3 cracks are a result of natural processes of valley flank widening and defacing of the outer edges of terrced slopes.

The disposition of the ground cracks in the study area shows that they dominantly fall in the areas occupied by non-plastic class and hence, the relation between the cracks and the Atterberg limits of the samples cannot be established. The pattern 1 ground cracks are present in the area with low moisture content range i.e., 11.15-15.48% (Table-12), whereas the pattern 2 and 3 ground cracks in the area cover wide range of 11.15 - 23.93% moisture content leading to no inference (Table-11). However, it indicates rapid draining of the soil particles and the same is corroborated by the outcomes of the preliminary report of NGRI, which categorically stated that the Joshimath subsidence was a dewatering phenomenon, which is continuing (NGRI 2023).

An insight into the position of the ground cracks vis-à-vis void ratio, porosity and permeability of the soil samples (Table-13) reveals that the ground cracks developed following the event of burst of water, are present in the area with low void ratio (0.58-0.66), low porosity (0.36-0.39) and low permeability (1.848×10^{-6}-2.416×10^{-6}). The other

International Journal of Engineering Research & Technology (IJERT)
ISSN: 2278-0181
Vol. 14 Issue 03, March-2025

ground cracks in the area cover wide range of void ratio (0.58-0.89), porosity (0.36-0.47) but low permeability (1.339×10^{-6}-4.058×10^{-6}). Although the ground cracks are specifically related with low permeability but the available data is limited for 13 plastic soil samples only, which are scattered within pervious sandy soil.

Table -12: Correlation of ground cracks with moisture content and Atterberg limits.

Crack Time	Moisture content (%)	Shrinkage Limit	Shrinkage Ratio	Plastic limit	Plasticity Index	Liquid Limit
No. of samples	32	14	14	14	14	14
Range in all the samples	(9.24-30.76)	(15.45-21.45)	(1.67-1.89)	(17.18-25.46)	(4.08-7.82)	(22.99-30.71)
Area affected by Pre-January 2023 cracks	11.45-23.93	16.58-18.24	1.78-1.85	17.68-22.18	5.57-6.56	23.56-27.94
Area affected by January 2023 cracks	11.15-15.48%	15.80-16.94	1.81-1.85	19.90-20.33	6.48-7.18	26.38-27.42
Area affected by July-August 2023 cracks	14.66-16.92	17.09-17.79	1.79-1.80	20.10-21.12	6.09-6.68	26.24-27.79
Range of parameter with ground cracks	11.15-23.93	15.80-18.24	1.78-1.85	17.68-22.18	5.57-7.18	23.56-27.94
No. of sample within the range	25	06	06	07	07	07
No. of sample out of range	07	08	08	07	07	07

The above inferences tend to suggest breach of layers with low permeability located within the pervious soil/overburden during ground distress, which lead to sudden draining of the soil in the aftermath of the burst of water noticed at Marwadi (J.P. Colony) in the lower part of the hill slope. The sudden draining of the water from the interstitial spaces between the soil grains clearly leads to development of tensional stresses which forces the soil particles to collapse and thus resulting into the tensional ground cracks as noticed in Sunil gaon, Manohar bagh, Singdhar and Marwadi areas of the middle part of the hill slope.

Table -13: Table showing correlation of ground cracks with void ratio, porosity and permeability.

	Void Ratio	Porosity	Permeability
Range	(0.48 - 1.13)	0.32 - 0.53)	($0.893*10^{-6}$-$11.3*10^{-6}$)
Area affected by Pre-January 2023 cracks	0.62 - 0.89	0.38-0.47	$1.339*10^{-6}$-$4.058*10^{-6}$
Area affected by January 2023 cracks	0.58 - 0.66	0.36-0.39	$1.848*10^{-6}$-$2.416*10^{-6}$
Area affected by July-August 2023 cracks	0.59 - 0.73	0.36-0.42	$1.850*10^{-6}$-$3.423*10^{-6}$
Range of cracks	0.58 - 0.89	0.36-0.47	$1.339*10^{-6}$-$4.058*10^{-6}$
Total size	32	32	13
Within range	22	20	04
Out of range	10	12	09

A clear outcome of the analysis of the data pertaining to the specific gravity of the samples (Table 14) is that the ground subsidence cracks developed during the event of 2nd January, 2023 are present in the area with soils having relatively high specific gravity range i.e., 2.66-2.71% wwhereas the other ground cracks (Old ones) in different parts of Joshimath exhibit a wide range of 2.58-2.71% of specific gravity thus leading to no direct correlation.

Table 14: Correlation of areas around ground cracks with specific gravity, dry and wet density of the matrix material.

	Specific Gravity	Dry Density	Wet Density
No. of samples	45	32	32
Range	(2.46-2.73)	(1.23-1.82)	(1.52-2.05)
Area affected by Pre-January 2023 cracks	2.58-2.70	1.40-1.63	1.72-1.90
Area affected by January 2023 cracks	2.66-2.71	1.62-1.71	1.84-1.93
Area affected by July-August 2023 cracks	2.62-2.68	1.55-1.65	1.78-1.94
Range of parameter with ground cracks	2.58-2.71	1.40-1.71	1.72-1.94
No. of sample within the range	36	19	21
No. of sample out of the range	09	13	11

International Journal of Engineering Research & Technology (IJERT)
ISSN: 2278-0181
Vol. 14 Issue 03, March-2025

The distribution of shear strength parameters of the different matrix samples tends to indicate a particular pattern vis-à-vis the locations of ground cracks in Joshimath area (Table-15). The ground cracks developed in the event of 2nd January, 2023 are present in the soil with low cohesion (5.01-10.59) and high friction angle (39.1°-42.22°) and the area affected by this event covers 70.65% slope which has <35° angle and 29.35% slope which has >35° slope. It is evident that slope angle in majority of the affected area was less than 35° which is lower than the internal angle of friction of the soil present in the affected zone. Nearly, similar correlation is present between the friction angle and slope angle with the ground cracks of pre-January and post-January, 2023 events, however, the percentage of relatively steeper slope (>35°) is comparatively high in the pre and post events as compared to January 2023 event.

Table 15. Position of ground cracks with cohesion, friction angle and slope area affected.

	Cohesion	Friction angle	Slope affected by ground cracks	
Total size	45	45	--	--
Range	(0-27.5)	(32.6-46.8)	<35° slope	>35° slope
Area affected by Pre-January 2023 cracks	0.10-21.60	33.49-43.11	63.48%	36.52%
Area affected by January 2023 cracks	5.01-10.59	39.1-42.22	70.65%	29.35%
Area affected by July-August 2023 cracks	7.83-15.99	39.81-42.94	64.32%	35.68%
Range of parameter with ground cracks	0.10-21.60	33.49-43.11	63.48-70.65%	29.35-36.52%
No. of sample within the range	33	33	--	--
No. of sample out of the range	12	12	--	--

It is thus amply clear that the ground subsidence witnessed in Sunil, Singdhar, Manoharbagh and Marwadi area (cracks following the 2nd January 2023 event) was a result of fissures in a soil with low cohesion. The sudden withdrawal of water from the interstitial spaces of the cohesion less matrix led to the collapse of inter-granular bond, which culminated in the form of tension cracks on the ground, in a NNW-SSE alignment between Marwadi and Sunil. The friction angle, although higher for these soils but it did not have any role in the ground subsidence. The friction angle would have played an important role, had there been a typical slope failure along a predefined failure plane or slip circle.

10. CONCLUSIONS:

The fast pace of development with a demand for more construction and infrastructural development is putting a lot of ecological stress on the hilly areas across the globe where there is paucity of flatter ground and the scenario becomes more so critical in a young and dynamically evolving and seismically sensitive higher Himalayan terrain like Joshimath. Almost all the human settlements and spots of tourist attraction in higher Himalayan region are located over the hill slopes occupied by thick overburden which is either is an old slide debris or a morainic dump of a retreating glacier and in either case the slope forming material is highly heterogeneous in nature.

The spatial distribution of ground cracks and their relation with the geomechanical properties of the soil brings out a significant prognostication that because of the highly heterogeneous nature of the overburden material on the Joshimath hill slope there is no possibility of a large global slip plane that can result in a circular failure engulfing major part of the township. The distress features and subsidences as noticed in different parts of Joshimath area are widely spaced temporally, have entirely different typology and also differ significantly in temporal existence. The middle lower part of the hill slope specially to the west of the geomorphic high i.e. Singdhar high, is having maximum thickness of overburden which is saturated in nature, as exhibited by the occurrence of innumerable springs, is more vulnerable to deep tensional ground cracks of slightly longer continuity (as noticed during the incidence of January 2023) as compared to the upper part of hill slope and the eastern part of middle slopes.

Careful identification/delineation of pattern 2 and pattern 3 cracks emerging in future holds the key for mitigation and subsequent treatment in the affected area. The study has clearly brought out all the three patterns of cracks (as noticed till July 2023) over the Joshimath hill slopes which should be very helpful to plan any mitigation and treatment measures that need to be adopted at these locations.

For future construction activities the authorities should avoid the areas occupied by coarse grained, non plastic, graded/poorly graded SM and SM-CL class soils which have high porosity and high permeability with a high void ratio. The upper part of the hill slope i.e. part located between Auli and Sunil gaon should not be disturbed considering the saturated nature of soil.

International Journal of Engineering Research & Technology (IJERT)
ISSN: 2278-0181
Vol. 14 Issue 03, March-2025

The present study has established that a carefully planned and executed scientific study with geotechnical testing of the soil samples can lead to precise identification of the cause and mechanism of ground distress features in a hill slope occupied by a thick pile of overburden/soil mass. Further, the present study corroborated that the land deformation in the region is primarily attributed to uncontrolled anthropogenic activities, infrastructural development, along with inadequate drainage systems [98]. Therefore the results of this study can be replicated successfully for other hill townships with similar nature of slope forming material and drainage characteristics, particularly in the higher Himalayan region.

ACKNOWLEDGEMENT

Authors are also thankful to Director General, Geological Survey of India for giving the opportunity to work in such a terrain and facilitating this research work.

REFERENCES:

[1] Gariano S. L. and Guzzetti F., Landslides in a Climate Change, Earth Science Reviews, Science Direct, 2017, pp 228-240, http://dx.doi.org/10.1016/j.earscirev.2016.08.011
[2] Petley, D., Global Patterns of Loss of Life from Landslides. Geology, 2012, 40, 927-930. https://doi.org/10.1130/G33217.1
[3] Moreiras, S. M., Climatic effect of ENSO associated with landslide occurrence in the Central Andes, Mendoza Province, Argentina, Landslides, 2005, 2, 53–59, https://doi.org/10.1007/s10346-005-0046-4,
[4] Petley, D.N., Hearn, G.J., Hart, A., Rosser, N.J., Dunning, S.A., Oven, K. and Mitchell, W.A., Trends in Landslide Occurrence in Nepal. Natural Hazards, 2007, 43, 23-44. https://doi.org/10.1007/s11069-006-9100-3
[5] Bennett, G. L., Miller, S. R., Roering, J. J., and Schmidt, D. A., Landslides, threshold slopes, and the survival of relict terrain in the wake of the Mendocino Triple Junction, Geology, 2016, 44, 363–366, https://doi.org/10.1130/G37530.1,
[6] Guha-Sapir, D., Below, R., and Hoyois, P. H., EM-DAT: International Disaster Database, Université Catholique de Louvain, Brussels, Belgium, 2018, http://www.emdat.be,
[7] Kinde, M., Getahun, E., Jothimani, M., Geotechnical and slope stability analysis in the landslide-prone area: A case study in Sawla – Laska road sector, Southern Ethiopia, Scientific African, 2024, 23, ISSN 2468-2276, https://doi.org/10.1016/j.sciaf.2024.e02071
[8] Petley, D.N., The mechanics and landforms of deep-seated landslides. In: Brooks, S., Anderson, M. (Eds.), Advances in Hillslope Processes. Wiley, Chichester,1996, pp. 823–835
[9] Valdiya, K. S. (1985). Himalayan transverse faults and their tectonic implications. Current Science, 1985, 54(12), pp 508–513.
[10] Pant, G., Maraseni, T., Apan, A., & Allen, B. L., Climate change vulnerability of Asia's most iconic megaherbivore: greater one-horned rhinoceros (Rhinoceros unicornis). Global Ecology and Conservation, 2020, 23, e01180.
[11] Bahuguna H. Kaistha, M. K., Singh, B. Das S. Mushtaq T. and Rana H., Preliminary Report on the Recent Event of Ground Subsidence at Joshimath, District Chamoli, Uttarakhand. 2023, Unpublished Preliminary Report of Geological Survey of India.
[12] Chasie M. Das S. Verma D. Singh Y. and Mushtaq T., Report on "Meso scale (1:5000) Geological and Geotechnical investigation of Joshimath Township, Chamoli district, Uttarakhand". 2024, Unpublished Report of Geological Survey of India
[13] Atkinson, Edwin T. (1886) The Himalayan Gazetteer. Volume 3. Part 1. The Himalayan Districts of the North Western Provinces of India. Volume XII of the Gazetter N.W.P.
[14] Heim, A., & Gansser, A., Central Himalaya: Geological observations of the Swiss expedition, 1936. Gebrüder Fretz.
[15] Mishra, M.C. (1976). High-Level Committee Report on Joshimath Sinking. Dehradun, India: Government of Uttarakhand.
[16] Sundriyal, Y., Kumar, V., Chauhan, N., Kaushik, S., Ranjan, R., & Punia, M. K., The northwest Himalaya towns slipping towards potential disaster. Natural Hazards and Earth System Sciences, 2023, 23, 1425–1431. https://doi.org/10.5194/nhess-23-1425-2023
[17] Sati, S.P., Sharma, S., Juyal, N, "Towards Understanding the Cause of Soil Creep and Land Subsidence around Historical Joshimath Town, Uttarakhand Himalaya", 2022, Report submitted to JBSS
[18] Garg, S., Karanam, V., & Motagh, M., Monitoring and Understanding Land Subsidence in Joshimath: An InSAR and Ground-based Study. EGU General Assembly 2023, Vienna, Austria, 2023, EGU23-15976, pp 23–28.
[19] CBRI, Mitigation, recovery & reconstruction of subsidence zone in Joshimath: safety assessment of buildings, 2023.
[20] Petley, D.N. Landslides and Engineered Slopes: Protecting Society through Improved Understanding. In: Eberhardt, E., Froese, C., Turner, K. and Leroueil, (eds) 2012. Landslides and Engineered Slopes, CRC Press, Canada
[21] Seismotectonic Atlas of India and Its Environs, 2000, published Geological Survey of India (GSI).
[22] Singh, P.K., Singh, T.N. and Singh, D.P., A Study of the Effect of Fault Plane on Slope Stability of OpencastMine by Equivalent Material-Modelling, MINETECH, 1998, pp. 37-44.
[23] Singh, T.N., Kumar, S. and Singh, D. P., Analysis of Toppling failure in Sandstone Quarry of Mizoram, Inst. Of Eng. (Mining), 1999, pp. 16-19
[24] Singh, T.N. and Monjezi, M., Slope Stability Study in JointedRockmass - A Numerical Approach, Min.Eng. Jr., 1(10), 2000, pp. 12-13.
[25] Singh, T.N., Gulati, A., Dontha, L. and Bhardwaj, V., Evaluating cut slope failure by Numerical Analysis – A Case Study, Natural Hazards, 2008, 47, pp.263-279
[26] Abebe,B. F., Dramis, G. Fubelli, M. Umer, A. Asrat, Landslides in the Ethiopian highlands and the Rift margins, J. Afr. Earth Sci. 2010, 56 (4–5) pp. 131–138, https://doi.org/10.1016/j.jafrearsci.2009.06.006.
[27] Kainthola, A., Verma, D., Gupte, S. S., Singh, T. N., A Coal Mine Dump Stability Analysis —A Case Study, Geomaterials, 2011, 1, 1-13 doi:10.4236/gm.2011.11001
[28] Kainthola, A., Verma, D., Gupte, S. S., Singh, T. N., Analysis of failed dump slope using limit equilibrium approach, 2011, Mini. Engg. Jour, 12 (12), pp. 28-32
[29[Kainthola, A., Verma, D., Thareja, R., Singh, T. N., A Review on Numerical Slope Stability Analysis International Journal of Science, Engineering and Technology Research 2013, 2 (6), pp. 1315-1320

International Journal of Engineering Research & Technology (IJERT)
ISSN: 2278-0181
Vol. 14 Issue 03, March-2025

[30] Verma, D., Kainthola, A., Singh, T. N., Thareja, R., Influence of water content on Geotechnical Properties of Deccan Basalt, Maharashtra, India, International Research Journal of Geology and Mining (IRJGM) (2276-6618) 2014, 4(4) pp. 122-132,DOI: http:/dx.doi.org/10.14303/irjgm.2014.024
[31] Kainthola, A., Singh, P.K., Singh, T N., Stability investigation of road cut slope in basaltic rockmass, Mahabaleshwar, India, Geosci. Front. 2015, 6 (6) pp. 837–845.
[32] Mahanta, B., Singh, H.O., Singh, P.K., Kainthola, A., Singh, T.N., Stability analysis of potential failure zones along NH-305, India, Nat. Hazards 2016, 83 (1) pp.1341–1357
[33] Segoni, S., Leoni, L., Benedetti, A.I., Catani, F., Righini, G., Falorni, G., Gabellani, S., Rudari, R., Silvestro, F., Rebora, N., Towards a definition of a real-time forecasting network for rainfall induced shallow landslides. Nat Hazards Earth Syst Sci 2009, 9:2119–2133
[34] Jia, N., Mitani, Y., Xie, M., Djamaluddin, I., Shallow landslide hazard assessment using a three-dimensional deterministic model in a mountainous area. Comput Geotech, 2012, 45(2012):1–10
[35] Mercogliano, P., Segoni, S., Rossi, G., Sikorsky, B., Tofani, V., Schiano, P., Catani, F., Casagli, N., Brief communication: a prototype forecasting chain for rainfall induced shallow landslides. Nat Hazards Earth Syst Sci, 2013, 13:771–777
[36] Carrara, A., Crosta, G., Frattini, P., Comparing models of debris-flow susceptibility in the alpine environment. Geomorphology, 2008, 94:353–378
[37] Baroni, G., Facchi, A., Gandolfi, C., Ortuani, B., Horeschi, D., Van Dam, J.C., Uncertainty in the determination of soil hydraulic parameters and its influence on the performance of two hydrological models of different complexity Hydrol. Earth Syst Sci, 2010, 14:251–270
[38] Park, H. J., Lee, J.H., Woo, I., Assessment of rainfall-induced shallow landslide susceptibility using a GIS-based probabilistic approach. Eng Geol, 2013, 161:1–15
[39] Lutenegger, A., J., Halberg, G.R., Borehole shear test in geotechnical investigation. Special technical Publ. Am Soc Test Mater, 1981, 740:566–578
[40] IIT Roorkee, The Geotechnical Investigations for determining the Shear Strength Characteristics and Bearing Capacity of the Soil in the Joshimath Region, Department of Earthquake Engineering Indian Institute of Technology Roorkee, Uttarakhand, INDIA, 2023, https://usdma.uk.gov.in/PDFFiles/IITR.pdf
[41] NGRI, Geological & Geotechnical studies to understand shallow subsurface strata at Joshimath, Chamoli, Uttarakhand, CSIR-National Geophysical Research Institute Uppal Road, Hyderabad, 2023, https://usdma.uk.gov.in/PDFFiles/NGRI.
[42] Komadja, G.C., Pradhan, S.P., Roul, A.R., Adebayo, B., Habinshuti, J.B., Glodji, L.A. and Onwualu, A.P., Assessment of stability of a Himalayan road cut slope with varying degrees of weathering: A finite-element-model-based approach. *Heliyon*,2020, *6*(11).
[43] Summa, V., Margiotta, S., Medici, L. and Tateo, F., Compositional characterization of fine sediments and circulating waters of landslides in the southern Apennines–Italy. *Catena*, 2018, *171*, pp.199-211.
[44] Getahun, E., Qi, S.W., Guo, S.F., Zou, Y. and Liang, N., Characteristics of grain size distribution and the shear strength analysis of Chenjiaba long runout coseismic landslide. *Journal of Mountain Science*, 2019, *16*(9), pp.2110-2125.
[45] Li, Z., Liu, Z., Cheng, P., & Li, Z., Micro-characteristics and meso-shear mechanism of the soils of a slip zone in a landslide. *Mechanics of Advanced Materials and Structures*, 2021, *29*(21), pp. 3122–3133. https://doi.org/10.1080/15376494.2021.1887417
[46] Sidle, R.C., Pearce, A.J., Loughlin, C.L.O., Hillslope stability and land-use. American Geophysical Union, Washington, DC, 1985, p 125
[47] Kitutu, M.G., Muwanga, A., Poesen, J., Deckers, J.A., Influence of soil properties on landslide occurrence in Bududa district, Eastern Uganda. Afr J Agr Res 2009, 4(7) pp.611–620
[48] Zung, A.B., Sorensen, C.J., Winthers, E., Landslide soils and Geomorphology in Bridger/Teton ForestNorthwest Wyoming. Phys Geogr 2009, 30(6) pp.501–516
[49] Mugagga, F., Land use change, landslide occurrence and livelihood strategies on Mount Elgon slopes, eastern Uganda. Unpublished PhD thesis, Nelson Mandela Metropolitan University, Port Elizabeth, 2011
[50] Van der Merwe, D.H.,The prediction of heave from the plasticity index and the percentage clay fraction of soils. Trans South Afr Inst Civil Eng 1964, 6(6):103–107
[51] Baynes, F.J., Anticipating problem soils on linear projects. In: Conference proceedings on problem soils in South Africa, 2008, pp 9–21
[52] Selby MG (1993) Hillslope materials and processes. Oxford University Press, New York
[53] Collettini, C., Niemeijer, A., Viti, C. and Marone, C., Fault zone fabric and fault weakness. *Nature*, 2009, *462*(7275), pp.907-910.
[54] Soto, J., Galve, J.P., Palenzuela, J.A., Azañón, J.M., Tamay, J. and Irigaray, C., A multi-method approach for the characterization of landslides in an intramontane basin in the Andes (Loja, Ecuador). *Landslides*, 2017, *14*, pp.1929-1947.
[55] Schäbitz, M., Janssen, C., Wenk, H.R., Wirth, R., Schuck, B., Wetzel, H.U., Meng, X. and Dresen, G., Microstructures in landslides in northwest China–Implications for creeping displacements?. *Journal of Structural Geology*, 2018, *106*, pp.70-85.
[56] Prakasam, C., Nagarajan, B. and Kanwar, V.S., Site-specific geological and geotechnical investigation of a debris landslide along unstable road cut slopes in the Himalayan region, India. *Geomatics, Natural Hazards and Risk*, 2020, *11*(1), pp.1827-1848.
[57] Nguyen, B.-Q.-V., Lee, S.-R., Kim, Y.-T., Spatial probability assessment of landslide considering increases in pore-water pressure during rainfall and earthquakes: Case studies at Atsuma and Mt. Umyeon, 2020, 187, 104317, DOI: 10.1016/j.catena.2019.104317
[58] Pei, X., Li, Y., & Xu, Q., Influence of weathering on the mechanical properties of rock and its implications for slope stability: A case study. *Engineering Geology*, 2020, pp.271, 105607
[59] Biondino, J., Conforti, M., & Buttafuoco, G., Weathering and its effect on the geomechanical properties of rocks in slope stability assessments. Geosciences, 2020, 10(12), pp.485.
[60] https://www.gsi.gov.in/webcenter/portal/OCBIS
[61] Gansser A., 1964. Geology of the Himalayas, Wiley-Interscience, New York.
[62] Gansser A., The geodynamic history of the Himalaya, in Zagros-Hindu Kush-Himalaya Geodynamic Evolution, Geodyn. Ser., 1981, vol. 3, edited by H. K. Gupta, and F. M. Delany, , pp. 111–121, AGU, Washington, D. C.
[63] Le Fort, P., Himalayas: The collided range. Present knowledge of the continental arc. American Journal of Science, 1975, 275(A), pp. 1–44
[64] Hodges, K. V.,Tectonics of the Himalaya and southern Tibet from two perspectives. Geological Society of America Bulletin, 2000, 112(3), pp. 324–350
[65] Singh, A., Chowdhary, G. R., Soil Engineering in Theory and Practice, 1990

International Journal of Engineering Research & Technology (IJERT)
ISSN: 2278-0181
Vol. 14 Issue 03, March-2025

[66] ASTM D6913/D6913M-17: This standard outlines the procedure for particle-size distribution (gradation) of soils using sieve analysis. It covers the determination of soil particle sizes ranging from 3 inches (75 mm) to the No. 200 (75 µm) sieve.
[67] BS 1377-2:1990: This British Standard specifies methods of test for soils for civil engineering purposes, including procedures for determining the particle size distribution by sieving.
[68] AS 1289.3.6.1-2009: This Australian Standard details the method for the determination of the particle size distribution of a soil using standard sieves.
[69] ASTM D7928-17: "Standard Test Method for Particle-Size Distribution (Gradation) of Fine-Grained Soils Using the Sedimentation (Hydrometer) Analysis." This standard provides the procedure for analyzing particles smaller than the No. 200 sieve using hydrometer analysis
[70] Holtz, R.D., & Kovacs, W.D., An Introduction to Geotechnical Engineering. Prentice-Hall, 1981.
[71] Chang, D. S., & Zhang, L. M., Debris flow induced by rainfall infiltration: A review. Journal of the Japanese Geotechnical Society, 2013, 53(2) pp. 190–207.
[72] Kenney, T.C., Lau, D., Internal stability of granular filters. Canadian Geotechnical Journal, 1985, 22(2) pp. 215–225.
[73] Schuler, U., How to deal with the problem of suffusion, Research and Development in the Field of Dams. SNCLD, Crans-Montana, Switzerland, 1995, pp. 145–159.
[74] Wan, C. F., and Fell, R., Assessing the potential of internal instability and suffusion in embankment dams and their foundation. Journal of Geotechnical and Geoenvironmental Engineering, 2008, 134(3), pp. 401–407. DOI: [10.1061/(ASCE)1090-0241(2008)134:3(401)]
[75] Fonseca, J., O'Sullivan, C., Coop, M. R., and Lee, P. D., Non-invasive characterization of particle morphology of natural sands. Soils and Foundations, 2012, 52(4), 712–722. DOI: [10.1016/j.sandf.2012.07.011]
[76] Fell, R., & Fry, J. J., State of the Art Review of Internal Erosion of Dams and Their Foundations. In: Internal Erosion of Dams and Their Foundations, Taylor & Francis Group, 2007, pp. 1-24
[77] Kezdi, A., Increase of Protective Capacity of Flood Control Dikes. Department of Geotechnique. Technical University, Budapest, Hungary. Report no. 1 (in Hungarian), 1969
[78] Li, M., & Fannin, R. J., A theoretical formulation for internal stability of cohesionless soil. Canadian Geotechnical Journal, 2008, 45(4), 511–524. DOI: 10.1139/T07-112
[79] Istomina, V.S., Filtration Stability of Soils. Gostroizdat, Moscow, Leningrad (in Russian), 1957
[80] Burenkova, V.V., Assessment of suffusion in non-cohesive and graded soils. Proceedings of Filters in Geotechnical and Hydraulic Engineering, Karlsruhe, Germany, 1993, pp.357−360.
[81] Roy, S., & Dass, G., Statistical models for the prediction of shear strength parameters at Sirsa, India. International Journal of Civil and Structural Engineering, 2014, 4(4), pp. 483–498
[82] Ameratunga, J., Sivakugan, N., & Das, B. M., Correlations of Soil and Rock Properties in Geotechnical Engineering. Springer, 2016.
[83] Kaniraj, S.R., Design Aids in Soil Mechanics and Foundation Engineering, McGraw Hill Education (India) Private Limited, New Delhi, 1988.
[84] Bureau of Indian Standards (BIS). IS: 2720 (Part 5) – 1970: Methods of Test for Soils – Part 5: Determination of Liquid and Plastic Limit. Bureau of Indian Standards, New Delhi, India, 1970
[85] ASTM D4318, Standard Test Methods for Liquid Limit, Plastic Limit, and Plasticity Index of Soils
[86] British Standard BS 1377-2:2022, "Methods of Test for Soils for Civil Engineering Purposes – Part 2: Classification Tests and Determination of Geotechnical Properties
[87] Australian Standard AS 1289.3.2.1-2009, titled "Methods of Testing Soils for Engineering Purposes, Method 3.2.1: Soil Classification Tests—Determination of the Plastic Limit of a Soil—Standard Method, 2009
[88] Indian Standard IS: 2720 (Part 6) – 1972, titled "Methods of Test for Soils: Part 6 Determination of Shrinkage Factors, 1972
[89] Prakash, K., & Sridharan, A., Free swell ratio and clay mineralogy of fine-grained soils. Geotechnical Testing Journal, 2004, 27(2), pp. 220–225. DOI: 10.1520/GTJ11320
[90] Burmister, D.M., Principles and techniques of soil identification. In: Proceedings of annual highway research board meeting, National Research Council, Washington, DC, 1949, 29, pp 402–433
[91] Casagrande, A., Classification and identification of soils. ASCE Trans, 1948, 113 pp. 901–930
[92[Howard, A. K., Modulus of Soil Reaction Values for Buried Flexible Pipe. Journal of the Geotechnical Engineering Division, 1977, 103(1), 33–43.
[93] Burmister, D. M., The general theory of stresses and displacements in layered soil systems. Journal of Applied Physics, 1949, 16(2), pp.89–94.
[94] Nayak, N.V., Christensen, R.W. Swelling Characteristics of Compacted, Expansive Soils. *Clays Clay Miner.* **19**, 251–261 (1971). https://doi.org/10.1346/CCMN.1971.0190406
[95] Terzaghi, K., Peck, R. B., & Mesri, G., *Soil Mechanics in Engineering Practice* (3rd ed.). Wiley-Interscience, 1996.
[96] https://www.cpc.ncep.noaa.gov/products/Soilmst_Monitoring/US/Soilmst/Soilmst.shtml
[97] https://www.worldweatheronline.com/joshimath-weather-averages/uttarakhand/in.aspx
[98] Awasthi, S., Jain, K., Sahoo,S., Kumar, R., Goswami,A., Joshi, G. C., Kulkarni, A. V., Srivastava, D. C., Analyzing Joshimath's sinking: causes, consequences, and future prospects with remote sensing techniques, Sci Rep, 2024,13,14,10876.doi:10.1038/s41598-024-60276-3